1983

Tests on simulated beam-to-column web moment connection details, February 1983

Abbas Pourbohloul

Xianru Wang

George C. Driscoll

Fracture of Moment Connections

TESTS ON SIMULATED BEAM-TO-COLUMN WEB MOMENT CONNECTION DETAILS

by

Abbas Pourbohloul
Xianru Wang
George C. Driscoll

This work has been carried out as part of an investigation sponsored by grants from American Iron and Steel Institute and the National Science Foundation (Grant No. CEE-8022041).

Department of Civil Engineering

Fritz Engineering Laboratory
Lehigh University
Bethlehem, Pennsylvania 18015

February 1983

LEHIGH/FL/469--7
Fritz Engineering Laboratory Report No 469.7

Table of Contents

List of Figures

List of Tables

ABSTRACT

The fracture failures of beam tension flanges observed in previous research work on beam-to-column web moment connections were the main impetus of the research on tension flange connection details at Lehigh University. In order to study the behavior of an isolated beam tension flange, a series of tension tests was conducted and results are presented in this report. Each connection detail was idealized as a simple tension plate, simulating the beam tension flange, and was attached through a connection plate to the web and flanges of a short length of wide flange member simulating a column.

Different tension flange connection details were simulated by variations in geometry and thickness of the connection plates, by variations in welding pattern, and by presence or absence of column web stiffeners opposite the tension flange.

Elastic and elastic-plastic finite element studies were conducted both to assist in the selection of details for experimental tests and to predict experimental behavior.

The experimental part of this project consisted of ten specimens including the five details for which the elastic-plastic finite element analysis had been conducted. Four specimens were tested with connection plates the same thickness as the beam flange plate and without stiffeners backing up the tension flange connection plate. Higher loads and more ductility resulted when connection plates were made longer to permit groove welds of beam tension flange to be placed a modest additional distance outside the plane of the column flange tips. A rectangular extension of the connection plate appeared to work as well as an extension which was tapered in width to improve the stress distribution. Three specimens were tested having both backup stiffeners and flange plates the same thickness as the beam flange. Even with a backup stiffener, a detail with the groove weld of the beam flange to the connection plate too near the plane of the column flange tips performed less well than two specimens with extended

connection plates.

Three specimens were tested with thicker connection plates designed to resist the effects of shear lag. Two of the three had no welds between the connection plate and the column web. Of these two, the one with a tapered, extended connection plate developed the full strength of the connected member. The companion detail had the tension flange plate groove weld to the connection plate immediately adjacent to the plane of the column flange tips. This specimen fractured in the heat-affected zone of the tension flange plate with the lowest margin above yield load of any specimen.

The third thick connection plate specimen had the connection plate welded both to the column web and flanges and a tapered extension of the connection plate allowed the flange plate groove weld to be farther from the plane of the column flange tips. The specimen exhibited good toughness and the joint developed the full strength of the flange plate.

Some of the simulated tension flange plates were cut so that the direction of applied stress was perpendicular to the direction of rolling and some were cut so that the applied stress was parallel to the rolling direction. In general, the Grade 50 steel plates pulled parallel to the rolling direction exhibited more ductility and toughness than those pulled perpendicular to the rolling direction.

In the simulated connection detail series, the connection plate fractures of the full-scale connection tests were not able to be duplicated. However, it was shown that certain details performed with better ductility and resistance to fracture. It was also shown that with proper proportions of welds and connection plates, a very good result can be obtained in a connection which has no weld connecting the connection plate to the column web.

1 INTRODUCTION

The concept for the current research program originated from a series of tests performed to investigate the strength of full-scale beam-to-column web moment connections [Rentschler, 1980].

1.1 Summary of Previous Work

In an effort to reduce to the absolute minimum the plate material, amount of welding, and extent of fabrication in beam-to-column joints, several specimens in a research program at Lehigh University were designed with no back-up stiffeners [Rentschler, 1980]. In these specimens, the beam was attached to the column in such a way as to bend the column about the weak axis. See Fig. 1. A sketch of a typical detail is given in Fig. 2.

In keeping with what has been done in such studies in the past, the specimens were designed to combine all of the "worst possible" situations:

- The connection plate was designed to yield at the same time that the full plastic moment of the beam was developed.
- Welds were proportioned according to the specifications--with no excess over requirements.
- The beam web connection to the column webs was proportioned for full shear yield on the web plate. Stresses in high-strength bolts corresponded to a bearing-type connection.

The results of two specimens gave marginal results. There was no difficulty with developing the service load, but the problem was with the lack of deformations in the vicinity of ultimate load. There were fractures prior to developing of significant rotation capacity. Fractures occurred in the tension flange connection plates, beginning where the weld terminated at the tips of the column flanges. Fractures continued into the base metal of the connection plates in the region between the column flanges. The metal involved was of normal strength and ductility, and the welds were typical welds.

Careful studies showed that there were no shortcomings in this regard [Driscoll, 1979].

Calculations showed that the failures took place due to stress concentrations at the point where the connecting plate (under high tension approaching the yield point) meets the column flange. Not only is there direct stress concentration, but at this point the stress is combined with two other tensile stresses--(1) that due to the through-thickness restraint (important for thick material) and (2) the tension stress built up as the tension plate tends to narrow, tending to pull the column flanges together (Poisson effect). This creates the ideal situation for the brittle fractures which occurred

Another experimental investigation has given an opportunity for comparison of results [Popov, 1969]. Web moment connections in that investigation also resulted in fractures at similar locations to those described above. However the specimens used much smaller structural members and were of ASTM A36 steel. Also those connections were subjected to reversed repeated loading into the inelastic range amounting to from 30 to 50 cycles of load. Fracture after that much straining would not be regarded as unexpected. However, fracture after one cycle of loading in the large-scale specimens must be looked upon with concern.

1.2 Objectives

In order to obtain information leading to a fuller understanding of the behavior and to improve the design of tension details in beam-to-column web moment connections, the current project in progress has the following objectives:

1. Determine the boundary conditions for premature fracture.
2. Determine methods for improving the stress condition and the ductility of this type of connection.
3. Determine the influence of geometrical effects such as thickness, slenderness, and restraints on behavior.

4. Determine methods suitable for design office use for proportioning connections and providing stiffening details which not only perform satisfactorily but may be fabricated economically by normal shop and field practice.

1.3 Expected Significance

Similar construction details are used in thousands of joints in steel-framed multistory buildings and other steel structures. In earthquake-resistant design, such joints are counted upon to perform in a ductile manner and prevent collapse of the structure if it is subjected to overloading by a severe earthquake. The web-type beam-to-column connections should be able to perform as well as do the flange-type beam-to-column connections under similar circumstances.

The results of this project will contribute to the knowledge and needs of other current and future research programs on the earthquake-resistant behavior of structural components and complete frames.(US-Japan Program)

1.4 Research Plan

The research plan was to first isolate the tension flange connection detail and then apply the results to a study of the whole connection.

A physical and mathematical model of the tension flange detail was formulated consisting of a short length of a column, a flange connection plate, and a plate simulating the tension flange of the beam. In this model, the principal variable was the flange connection plate. Variations in the shape, thickness, and pattern of welding to the column provided the range of different details studied. The connection plate and the simulated tension flange plate were to be fastened perpendicular to the web plane of a 4-foot long column stub at its center. This assemblage would be supported as a simple beam at the ends of the column stub. A tensile force which would create moment about the weak axis of the column would be applied on this

tension plate. Effects of the beam web, beam shear connection, and the beam compression flange were neglected in the preliminary model. This assumption, with a rudimentary analytical justification, was made in order to achieve an economical model for both computational and experimental purposes.

Theoretical Analysis

Up to the present time, two types of theoretical analysis have been conducted to prepare for the testing program.

Parametric Study

A parametric study of elastic stress distributions of several details was carried out using a linear finite element program [Bathe, 1974]. The parametric analysis was conducted as a first step, to evaluate the effect of different thicknesses and geometries of the flange connection plate on stress concentration. This analysis helped select appropriate details for a second step of analysis. A report on this study has been written and distributed to the Advisory Committee [Shen, 1981a].

Step-By-Step Analysis

An elastic-plastic step-by-step load-deflection analysis was carried out on a series of simulated tension flange connection details adopted from the results of the parametric analysis. Figure 3 shows layout and dimensions of the plates used in the elastic-plastic analysis. Case A represents most nearly one of the specimens that fractured in the full-scale beam-to-column web connection tests. Case B is the same detail, but with a 1-inch thick stiffener supplied. Both case A and B were analyzed with the joint of the simulated beam flange flush with the plane of the tips of the column flanges, although it would not be a suitable joint for welding. However, no specimens were fabricated this way. Case C has the connection plate tapered and extended 3 inches beyond the flange tips to move the joint

to the beam flange away from the zone of restraint between the column flanges.

Case D is essentially the same detail as case A, but a thicker 1-5/8 inch connection plate is used to reduce the stresses in the connection plate. Case E uses a 1-5/8 inch connection plate, but no weld is to be applied between the connection plate and the column web. Case F has the same detail as case C but has a thicker connection plate to investigate the effect of reducing the basic stresses. Case G was studied to observe the effect of an extended tapered connection plate not welded to the column web.

The analysis of these details was carried out through a step-by-step procedure using the linear finite element program SAP4 [Bathe, 1974]. The calculations provide predictions of stress and deflection up to the point where the simulated beam tension flanges become completely yielded. A report on this study has also been distributed to the Advisory Committee [Shen, 1981b]. That report contains step-by-step load-deflection curves, stress distributions, and sketches of yielding patterns.

Results contained in these two reports indicate the influence of change of detail on the distribution of yield stress patterns in connection plates and tension flanges. For example, Fig. 4(a) shows how yielding would spread into the region between the column flanges. Fig. 4(b) and (c) however, indicates how a connection plate of properly increased thickness forces the yielding to occur in the tension flange where the stress distribution is much less complex, and less likely to cause fracture.

2 PROGRAM OF TESTS

The test program was originally composed of ten different specimens. Details of those specimens are shown in Table 2. The first specimen was retested after a crack initiated at one of the tack welds and caused the failure of the tension plate. Detail D2 was dropped out of the test program. As will be discussed later, the main reason for using a thicker connection plate is to provide for a larger amount of material in order to reduce the magnitude of the shear lag phenomenon. This allows then the possibility of eliminating the fillet welds joining the column web to the connection plate. The descriptions of different specimens listed in Table 2 are as follows:

Specimen A (Test T1):

This test was a control test on which the comparison between the effect of various parameters on stress distribution was based. The thickness of the connection plate was one inch, the same as that of the tension plate. The connection plate was fillet welded all around its top and bottom periphery to the column web and column flanges.

Specimen A-revised (Test T2):

This was a re-test of specimen A to investigate the effect of tack welds on the mode and location of failure. Tack welds were used to position the backing bar provided for applying the groove weld between the flange plate and connection plate. The re-test plan was proposed after it was concluded that tack welds might be responsible for crack initiation. To repair the specimen, a new flange plate was used and tack welds of the backing bar were made at the root ofthe groove weld where they could be incorporated into the final groove weld.

Specimen B (Test T3):

The benefits of using an extended connection plate were examined in this test. Both connection and tension plates had the same thickness.

Specimen C (Test T4):

A one inch thick connection plate was tapered with a 3:1 slope in the direction of applied load and it was groove welded to a tension plate of the same thickness.

Specimen D (Test T5):

This specimen had a 1-5/8 inch thick connection plate and there were no fillet welds at the column web-to-connection plate junction. This test specimen could show the possibility of eliminating the column web fillet welds through the use of a thicker connection plate which in turn could lead to less fabrication cost for this moment connection detail.

Specimen E (Test T6):

The connection plate had the same thickness and force boundary conditions as those in specimen D. However, the connection plate was tapered in width in an effort to assure a better stress distribution across the line of the groove weld.

Specimen A2 (Test T7):

The back-up stiffener in this specimen was used to relieve some of the stress concentrations at the column flange tip-to-connection plate junction by mobilizing the back portion of the column flanges. In this way, the column web could more effectively contribute to a better stress distribution in the connection plate across the column flange tips.

Specimen B2 (Test T8):

Extension of the connection plate and use of a back-up stiffener in this specimen provided a more favorable condition for stress distribution.

Specimen C2 (Test T10):

This specimen had a tapered connection plate and a back-up

stiffener. Although the stress distribution pattern in the connection plate within the column flanges was not expected to be much different from specimen B2, strain constraints at the reentrant corners of the connection plate were assumed to be reduced by tapering it. This would in fact have been beneficial were a crack to be initiated in this region.

Specimen E2 (Test T9):

The 1-5/8 in. thick connection plate in this specimen could reduce the stress concentrations at the column flange tips through carrying more stresses via the column web.

2.1 Test Setup

The test setup is shown schematically in Fig. 5. The upper portion of the test setup, namely the fixture, was similar to the test specimen such that a symmetrical loading condition could be maintained during testing. The fixture was much stronger than the specimens in order to prevent failure in this part of the test setup. A two inch thick tension plate was groove welded to a W14x257 column stub in such a way that the induced bending moment was about its strong axis. Two reusable end plates were bolted to both ends of the column stubs of the test fixture and test specimen.

The 5-million lb. Universal Testing Machine was used to furnish the required tensile force applied at the far ends of the flange tension plate and the fixture tension plate on a gripping length of two feet each. Fig. 6 shows a picture of a ready-to-test specimen placed in the testing machine.

2.2 Test Procedure

The testing procedure consisted of applying small increments of tensile forces to the far ends of the pulling plates. The load-deflection curve was plotted for a 17.0 inch long gage length. For comparison, the same gage length was used to draw the results of the

finite element analysis. To control and follow the behavior of the specimen, the load-deflection curve along with a load-strain curve of a critically-located strain rosette gage were plotted while testing was in progress. Small load increments of about 10 to 20 kips. were used at the beginning of each test to reduce the nonlinear behavior of the load-deflection curve in this region. This occurs frequently due to uneven or inadequate gripping.

About fifteen load increments, each equal to 50 kips. on the average, were applied until the yield load of the tension plate was reached at about 540.0 kips. Loading was stopped to take data readings in the linear range. Usually there was about a two minute elapsed time to arrive at a fairly equilibrated state. The required elapsed time in the strain-hardening region increased to 3 and 4 minutes for load values of about 600 kips and 700 kips respectively.

The time and the load value, before commencing a new loading step, were recorded after the yield load of the tension plate had been reached. Deflection gages were reset 4 times on the average in each test. In the last three tests, after removing the deflection gages and prior to the specimen failure, the elongation of the strain-hardened tension plate was recorded through changes of the machine head position with an accuracy of about 1/16 inch. The change in the head position at this stage of loading could well be attributed to the elongation of the ungripped length of the tension plate as there was little change in the load value from the time that deflection gages were removed until the failure of the tension plate.

3 PREPARATION FOR TESTS

3.1 Material Property Tests

Three different types of material property tests were carried out in order to determine the tensile strength and toughness of the material. ASTM A572 Grade 50 steel was selected for fabricating the specimens. A total number of seven tensile coupons were prepared and tested for two different thicknesses of the connection plate and two different rolling directions of the tension plate material. The tension plates originally provided by the fabricator had their rolling directions perpendicular to the pulling direction.[1] This was not a desirable orientation for tension plates as it does not simulate the real condition that exists in a rolled beam. In the second series of connection detail tests (series 2) tension plates with rolling directions parallel to the direction of the applied load were used. Tensile coupons of the second series are designated by letter "R" at the end of the specimen number. All coupons were 1.5 in. wide and had the same thickness as the tension plates from which they were prepared. Table 3 shows tensile properties of all of the coupons that were tested and a bar graph illustrating their yield and tensile strength is sketched in Fig. 7. The fractured surface of coupons with cross sectional dimensions of 1-1/2 x 1-5/8 was totally flat without any slanted surface while the 1.5 x 1.0 in. coupons demonstrated a typical cup-cone surface.

The Charpy impact tests were carried out for different notch orientations. The TL and LT type of Charpy specimens were machine cut from steels which had been used in fabrication of the first series of connection tests. Fig. 8 shows the Charpy impact energy versus temperature curves for the two groups which were tested. LT specimens were used for Charpy tests of the second series of connection detail experiments. Fig. 9 illustrates results of these tests which shows a

---

[1] The fabrication order did not specify orientation.

typical notch toughness behavior of an A572 steel [Novak, 1974].

3.2 Inspection and Repair of Welds

In repairing the defective groove welds and fabrication of new specimens, low-hydrogen electrodes were used. The electrode diameters and the preheating conditions for welding were in accordance with the AWS Welding Code requirements [American Welding Society, 1980]. The AWS Welding Code also requires that a transition region be provided between two plates with different thicknesses. This condition was met for those specimens which had a thicker connection plate than the tension plate.

To create the specimens for the second series of detail tests, the stub column sections of the first series were salvaged and reversed. A fresh detail of connection plate and tension plate was fabricated on the undamaged side. The connection plate on the damaged side was either burned away or burned to the proper dimension to serve as a backup stiffener.

In fabricating a new specimen by groove welding a connection plate to a single beveled tension plate, the tension plate rotates upon cooling of the groove weld due to a higher cocentration of weld deposits on the beveled side. In order to reduce this postwelding deflection of the tension plate, it was initially positioned at a small angle to the plane of the connection plate and toward the root of the groove weld. Then a backing bar was tack welded at the root of the groove weld. In this fashion, tack welds could be fused into the final groove weld. This procedure was carried out for those specimens of the second series which were fabricated in Fritz Engineering Laboratory. However, this was not the case for the prefabricated specimens in which tack welds had been applied directly on the outside surfaces of the tension and connection plates. These tack welds were removed after their deleterious effect on crack initiation was appreciated as a result of the first connection detail test.

The sizes of fillet welds were checked in each test before setting-up the specimens. The welds were also visually inspected by a welding technician to see if there was any visible crack or peripheral discontinuity of welds. A dye penetration test was used to check the groove weld of the second test. After the first project committee meeting in January 1982, ultrasonic testing of groove welds was carried out for the remainder of the specimens according to the committee recomendations.

Specimen C was the first one for which the groove weld was ultrasonically tested. A lack-of-fusion type of discontinuity was detected all along the root of the groove weld. Fig. 11 shows a sketch of the defect. To repair this groove weld the backing bar was removed via an air arc process. The backing bar dropped off the connected plates upon burning the tack welds. This showed the lack of fusion of the groove weld. The defective zones were ground by a pencil grinder and a series of weld passes was deposited to obtain adequate strength of the groove weld.

Ultrasonic testing of specimen D revealed two rejectable defects in different locations and depths of the groove weld. Those defects could have been introduced through entrapped weld slag, the so-called "cold lap" discontinuity, as well as a simple porosity in the weld. Fig. 12 illustrates the sizes and locations of those defects. The same repair processes were carried out as before.

The groove weld of specimen E contained three rejectable defects. A sketch of these weld defects is shown in Fig. 13. The backing bar was removed by the air arc process. Grinding of the groove weld root confirmed the validity of the ultrasonic test results. The groove weld was repaired by removing the defective zones and rewelding them.

Only one out of four specimens fabricated in the Fritz Laboratory welding shop had a rejectable discontinuity in the groove weld. This specimen which was used in test T10 had a cold-lap defect which was

about 1.75 in long and 0.75 in deep as is shown in Fig. 14. The same repair process was followed for this specimen.

Another problem with the prefabricated specimens was the end return of the fillet welds of the connection plate. Fillet welds at the junction of the connection plate and column flanges had been tied together at the column flange tips. Such a welding procedure is prohibited by the AWS Welding Code; however, the welds were left intact. Joining to the end returns was not practiced in those specimens that were fabricated in the laboratory shop.

3.3 Instrumentation

Strain rosette gages (SR-4 gages) were installed on the connection plate and backup stiffener, if there was any, in order to measure strains at different locations. The strain rosette layouts were different from each other because of the variation in specimen details. Fig. 15 and Table 4 provide a summary for visualization of the rosette gage pattern of each specimen. The numbers on each row represent the numbers of rosettes used in the corresponding rosette line. These rosette lines are designated alphabetically in Fig. 15. Rosettes on lines F and G were used to evaluate the effect of the backup stiffener in transferring stresses to the compression flanges of the column through column web interaction. Rosettes on lines B',C', D', and E' were used on connection plates which were thicker than the corresponding tension plates. This was done in order to consider the bending effect of the pulling force on the connection plate. The bending moment was induced since the bottom side of the tension flange was flush with the connection plate which in turn creates an eccentricity of the resultant stresses. Fig. 16 shows an overall view of a cantilever gage which was used to measure the elongation of the gage lengths. Four 1/8 in. foil gages, constituting a full bridge circuit, were glued to each side of the two overhanging aluminum plates. Deflection of the cantilever arms could be measured by calibrating the strain readings displayed through a B&F Data Acquisition System. Roughly speaking, a cantilever gage may be

thought of as an oversized clip gage such as used in crack mouth opening measurements of a fracture toughness test. The accuracy of this cantilever gage in its linear range of operation is about 10^{-4} inches. A sketch of the deflection gage lengths is shown in Fig. 17. The gage lengths were chosen symmetrically on both sides of the tension and connection plates in order to diminish the effect of the initial curvature and rotation of the pulling plate on the gage elongation measurements. These measurements were carried out by using six cantilever gages on both sides of the specimen. The gage lengths which were used to plot the load-deflection curves of each test were the average of the total elongation of gage lengths "a" and "b" on both sides of the connection and tension plates.

4 TEST RESULTS

A listing of test numbers and specimen identification numbers for all tests is given in Table 1. Key information including the connection plate thickness, fracture loads, and ductility is given in Table 2 along with sketches of the specimen and fracture trace. Sketches of all specimens plus a bar chart giving the relative magnitudes of maximum loads are given in Fig. 22 and 23.

Load-deflection graphs for all specimens are given on Fig. 18 and 21. The graphs are spaced on each page so that they will best fit on the sheet and so that the relative magnitudes of behavior can be compared. Each graph is plotted as a solid line with data points up to the point where deflection gages were removed from the specimen in order to preserve the gages for further use. To give a conservative estimate of ductility, the curve was projected through its final two points up to the level of the maximum load registered on the testing machine. The true ductility was probably never less than this estimated value because the curves tend to level off when they near ultimate load. Some of the curves give data values all the way up to failure because fracture occurred while the deflection gages were still in place. Comparison of the complete curves with the extrapolated curves gives the impression that extrapolation is reasonable.

Comments on each individual test are given in the following paragraphs.

4.1 Description of the Behavior of Test Specimens

Test T1 (Type A with connection plate extending only 3/4 inch beyond column flange tips):

A load-deflection curve of Test T1 is given in Fig. 18. The maximum load occurred at 730 kips, equivalent to 73 ksi ultimate stress, about 35 percent greater than the nominal yield stress.

Fracture occurred after a fairly extensive elongation, over six times the elongation required for nominal yield of the tension flange, as shown in Fig. 18. The theoretical curve obtained from the elastic-plastic finite element analysis, computed up to the yield point, is plotted as a dashed line in the same figure. Whitewash had been applied to the specimen in order to observe flaking of mill scale caused by surface yielding of the specimen. However, very little whitewash flaking had been observed before the specimen failed abruptly with a loud noise. A close inspection of the fracture surface (as shown in Fig. 19) revealed that a crack had initiated at one of the outer tack welds and propagated rapidly across the flange tension plate. Fig. 20 shows the trace of the crack near the outer edge of the backing bar. The region near the tips of the column flanges where crack initiation had been presumed to be most probable, was not involved in the fracture.

Test T2 (Type A-revised with connection plate projecting only 1/2 inch beyond the column flange tips):

Fig. 18 shows the load-deflection curve of test T2. The dashed line is the estimated plot of the load-deflection curve after removing the linear variable displacement transformers (LVDT's). The deviation of the experimental curve from the theoretical curve which is shown in this plot is partly due to the initial rotation misalignment of the tension plate resulting from the groove welding process. Also, experimental error in the placement of the LVDTs was another reason for this inconsistency. Local yielding of the tension plate was indicated at a load level that was about 28 percent of the nominal yield load. The tension plate fractured at 730 kips followed by a loud noise. Although the fracture load was the same in both tests T1 and T2, the crack initiation site was different. It radiated from one of the edges of the tension plate in test T2 where stress concentration was the highest. The fracture surface was nearly flat and parallel to the groove weld. Table 2 shows the top view of the fractured specimen with the crack trace running from one edge of the tension plate to the other.

Test T3 (Type B with connection plate extended 3 inches beyond the column flange tips):

The experimental load-deflection curve of test T3 is shown in Fig. 18. Deflection gages were removed at 705 kips. The dashed line speculates the behavior of the specimen from this point on up to the fracture load which was 824 kips. The elongation of the gage length was about nine times that at the nominal yield load, that is 530 kips, which indicated fairly ductile behavior. Whitewash flaking started at 580 kips which was a little higher than the nominal yield load. Plastic deformation of the specimen was suddenly disrupted due to a fracture that initiated at one of the edges of the tension plate. Failure of the tension plate occurred through a cleavage process where chevron markings were pointed toward the crack source on the plate edge. Some slanted fracture surfaces could be recognized in the neighboring regions of the weldment which were associated with the ductility of the weld material. However, the rest of the fractured surface was flat. The fractured surface displayed shiny cleavage facets.

Test T4 (Type C with tapered connection plate extended 3 inches beyond the column flange tips):

The entire load-deflection curve up to the fracture load is shown in Fig. 18. The small shift in the curve at 400 kips was due to a major slip in end plate bolts which occurred during this loading step. This specimen had a deformation ratio of about six and the nominal stress of the tension plate was 75.6 ksi when the specimen was totally severed by fracture in the connection plate. Whitewash flaking started at around 590 kips and all of the mill scale had flaked off the tension plate at 686 kips. Because of a compact rosette layout that had been used for strain measurements and the surface grinding for their proper installation, the whitewashed region was relatively small and mostly on the central regions of the connection plate. This was a typical case in most of the tests, and hence no whitewash flaking was observed on the connection plate during the whole testing period. However, a little whitewash flaking could be noticed on the column web where it joined the connection plate and also at the tips

of the compression flanges of the column stub. No crack was detected prior to the abrupt failure of the tension plate. Chevron markings indicated that a crack had originated at one of the edges of the tension plate. A top view of the fractured connection plate showing the fracture trace is illustrated in Table 2. The fracture surface was predominantly flat with some slanted surfaces in regions that were close to the weldment.

Test T5 (Type D with 1-5/8 in thick connection plate welded to the column flanges only):

This specimen showed the lowest load-carrying capacity of any despite the groove weld repair that was mentioned in the previous section. A brittle fracture severed the tension plate in the vicinity of the groove weld at 590 kips. Not much whitewash flaking was observed prior to fracture. The deformation ratio was much smaller than those of the previous tests; it was about 1.71. The amount of plasticity in the tension plate was estimated by measuring the change in distances between punch marks that had been placed at a variable spacing within a twenty inch length, starting from the groove welding line. Plastic deformation was expected to be larger in regions farther from the groove weld where the effect of a two-dimensional state of stress has presumably vanished. The maximum plastic strain was less than 0.5% compared with the corresponding value of specimen C which was around 5%. A crack initiated at one of the edges of the tension plate and propagated rapidly across the tension plate. The cleaved surface was flat and some slanted surfaces had formed in regions near the weldment.

Test T6 (Type E with a thick tapered connection plate extended 3 inches, not welded to the column web):

Fig. 18 illustrates the load deflection curve for this specimen up to 760 kips with a dashed projection to the ultimate fracture load of 802 kips. The slight shift of the curve at 650 kips was due to a longer elapsed time taken for resetting the deflection gages. The average ultimate stress of the tension plate was 80.2 ksi with a deformation ratio of 6.81. Most of the whitewash flaking of the flange tension plate occurred at loads above 600 kips. At loads near

to 750 kips, some whitewash flaked off the column flange tips opposite to the connection plate and also on the far ends of the column flange where it had been bolted to the joining plates. This whitewash flaking was not comparable to that on the tension plate but enough to be distinguished from the other column flange and it occurred on the same side where a crack initiated. This specimen was the only one in the group with tension perpendicular to the direction of rolling that fractured at a distance away from the groove weld, that is about 27 in from the column flange tips.

Very small shear lips could be observed on the fracture surface whereas the rest of the shiny areas were relatively flat.

Test T7 (Type A2 with connection plate projecting only 3/4 inch beyond the column flanges and having a backup stiffener):

This was the first test on a specimen that had a tension plate with the rolling direction parallel to the applied load. This provided the specimen with a higher ductility as can be observed from the load-deflection curve shown in Fig. 21. The deformation ratio was 17.7 at 739 kips, the load at which deflection gages were removed. The fracture load was 762 kips which induced an average tensile stress on the tension plate of 76.2 ksi. Whitewash flaking was observed on the tension plate at 560 kips and all mill scale flaked off by the time that a load of 610 kips was reached. This was the only specimen in the series of tests with rolling direction of the tension plates parallel to the direction of stress that sustained a fracture in the vicinity of the groove weld. A crack initiated at one of the edges of the tension plate and propagated at a high speed, analogous to the preceeding six tests. The fracture surface was flat with very little evidence of shear lips on the tension plate edges.

Test T8 (Type B2 with connection plate extended 3 inches, and having a backup stiffener):

Fig. 21 illustrates the load-deflection curve up to 707 kips. The deformation ratio under this load was 10.17; however, if the load-deflection curve is extrapolated beyond this point as far as the fracture load of 795 kips, a conservative estimate of deformation

ratio of about 17.8 can be obtained. At 550 kips whitewash started to peel off the tension plate and flaking was completed at 630 kips. A distinct herringbone pattern of whitewash flaking was observed on the back side of the connection plate at a load of 750 kips.

A crack that originated from the edge of the tension plate and 15 inches away from the groove weld branched after it propagated for about 1 inch in the tension plate. The specimen fractured through the main crack before the secondary crack met the opposite edge of the tension plate. The fracture surface was flat with chevron markings pointing back to the crack origin. There was very little evidence of shear lips on the edges of the fractured tension plate.

Test T9 Type E2 with 1-5/8 inch-thick tapered connection plate extended 3 inches):

The deflection gages in this test were removed at 744 kips prior to the maximum load of 814 kips at which fracture occurred. The deformation ratios at these load levels were 9.72 and 16.4 with the latter obtained by extrapolation as a conservative estimate of the result had the gages remained in place. The load-deflection curve and an estimate of the specimen behavior beyond 744 kips are shown in Fig. 21 by solid and broken lines respectively. Most of the whitewash on the tension plate flaked off between loads of 560 kips and 630 kips. Also a small amount of whitewash peeled off the tip of the column flange opposite to the connection plate. The tension plate had undergone a large amount of plastic extension when fracture occurred. Cracks initiated on both edges of the tension plate at roughly 15 inches away from the tip of the column flanges. Although both cracks contributed to the fracture process and eventual separation of the two pieces of the tension plate, their different lengths suggested that they were not initiated simultaneously. Also the first crack branched out in its early stage of propagation. Chevron markings pointed to different directions on both fracture surfaces which were shiny and relatively flat.

Test T10 (Type C2 with backup stiffener and tapered connection plate extended 3 inches):

This specimen showed the largest plastic deformation of all ten experiments. The load-deflection curve of this specimen is plotted as the first curve in Fig. 21 along with other load-deflection curves in order to give a better picture of the specimen behavior. Deflection gages were dismounted at 787 kips where the deformation ratio was 29.6. The maximum load that was reached was 813 kips; however, fracture occurred at 650 kips after an apparent necking of the tension plate. Whitewash of the tension plate flaked off between loads of 577 kips and 608 kips. There was evidence of some yielding on the inside and outside of the column flanges close to the connection plate and backup stiffener. Crack initiation sites were at two different locations on the two edges of the tension plate. The first crack had a relatively straight trace whereas the second one that started later followed a quarter ellipse path which met the first one at mid-width of the tension plate. A top view of the fracture trace is shown in Table 2. The fracture surface at the point where the second crack initiated was a complete slanted surface without any flat region over a length of 1/2 inch. Both cracks had a flat surface with chevron markings pointing towards their initiation site.

5 DISCUSSION

At this point it is appropriate to discuss how the outcome of the theoretical and experimental investigations may be used to solve problems of design of connections and it is also appropriate to comment on how well the program has met its objectives. Included in the discussion will be comments on the properties of the materials and how the materials were used, on several aspects involving welds and welding, and on how the test results provide information useful for formulating design recommendations.

5.1 Material Properties

Two types of 50 ksi grade steel were used in the significantly stressed parts of the connection detail test specimens, A572 and A588. Tensile coupon tests and Charpy V-notch impact tests of both materials were consistent with normal values expected.

One unforseen experience involving the steel may have had an influence on the outcome of the experiments. For the first six tests, the 10 x 1 inch plate which simulated the beam tension flange was oriented so the direction of stress was perpendicular to the direction of rolling. In the order for 5-foot long pieces of 10 x 1 plate, no stipulation regarding rolling direction was made and pieces just happened to be cut perpendicular to the rolling direction. Rolled beam flanges in a beam-to-column connection would, of course, be stressed in the direction of rolling. There was some doubt as to whether the plates would fairly simulate the beam flanges. It was known that steel rolled plates have somewhat lower physical properties perpendicular to the direction of rolling. However, even these properties equal or exceed the standards for the material and the material is appropriate for use when stressed in either direction.

The originally-supplied plates were used for the first six tests conducted, but for the later tests it was decided to obtain replacement plates cut so they would be stressed in the direction of rolling. At the time 1-inch plates of A572 Grade 50 steel were not

available. Instead there was available a quantity of 1-1/8 inch plate of A588 Grade 50 steel which is usually acceptable as a substitute for A572 steel. To provide equal tension areas, the new plates were cut to a cross-section of 9 x 1-1/8 in.

From one aspect, neither the plates stressed parallel to the direction of rolling, nor those stressed perpendicular to the direction were a match for the flanges of a rolled structural shape. The flame-cut edges of the plates would all have tensile residual stresses equal to the yield stress of the plate whereas the flange tips of rolled structural shapes always have compressive residual stresses due to the rolling and cooling process. There was a concern that the presence of high tensile residual stresses would initiate premature fractures at the outer edges of the plates.

The eventual outcome of the tests showed that the fractures which occurred were not a function of flame-cut edges. There did appear to be a difference in the toughness of specimens with tension plates stressed parallel and perpendicular to the direction of rolling. However within each series, the results for particular types of specimen details were consistent with either type of tension plate as will be discussed in more detail later.

5.2 Welding Details

During the preparation for welding, decisions had to be made about the application of alternate options on welding details including tack welds, backing bars for groove welds, and end returnes on fillet welds.

End Returns of Fillet Welds

The four longitudinal fillet welds which fasten the sides of the connection plate to the column flanges would normally terminate at the tips of the column flanges. The AWS Structural Welding Code recommends that such welds be returned continuously around the corners for a distance at least twice the nominal size of the fillet welds.

There was concern that this practice, which would cause the meeting of the end returns of the fillet welds on the top and bottom of the plate, would lead to fracture of the plate because of "intersecting fillet welds." Efforts were made to terminate the end returns before they met in the test specimens. It has since been determined that smooth continuation of the end returns leading to a sound fillet weld along the full thickness of the connection plates does not constitute "intersecting fillet welds" of the type feared to cause fracture.

Backing Bars and Tack Welds

Backing bars were required for applying the groove welds needed to make the butt joints connecting the simulated beam tension flanges to the connection plates. Where the groove welds were applied in the fabrication shop, the backing bars were first tack-welded into place by six tack welds applied along the edges of the backing bars fastening them to the lower surfaces of the connection plate and flange plate. The backing bars and tack welds were left in place as is permitted in buildings. When the first test was made, it was obvious that fracture had initiated at the location of a tack weld. Discussion with the fabricator brought out the fact that for the same joint to be welded in the field, the tack welds would have been made from above and placed at the root of the groove where they would later be fused into the final groove weld. In this position, the tack welds should have less effect on crack initiation. The fractured zone on the first specimen was cut away and a new simulated tension flange was welded to the connection plate using a new backing bar and the revised location for the tack welds. The test load was the same in the re-test possibly showing that the tack welds did not significantly decrease the static tensile strength of the joint even though they did dictate the location of crack initiation once it was time for the specimen to fracture.

The tack welds on the remaining four specimens of the first test series were ground away. The backing bars were removed from three of the four as well in order to allow repairs to be made to the groove welds.

In the series of specimens using 9 x 1-1/8 inch tension flange plates, all tack welds were placed at the root of the groove and the backing bars were allowed to remain in place after the groove welds were completed.

Performance of Repaired Welds

In a previous section the use of sonic testing to locate weld flaws and the subsequent repairs were discussed. The accuracy with which the flaws were located was remarkable. In most cases there was no sign of the flaw until the grinding wheel reached the depth identified by the sonic test. However, it appears that success in using the sonic tests depends very much on the skill of the operator and having simple joints.

The success of the weld repair is evident in that two specimens developed the full section of the tension plate (E and C2) and a third (C) had its final fracture in the connection plate between the groove weld and the column. The final repaired specimen (D) seemed to be consistent with those with similar details (A, A_{rev}, A2) where the connection plate was not extended.

Based on the total of ten connection detail tests it is clear that those specimens with extended connection plates have better toughness and ductility and should be preferred in design against earthquake, even though the other connection types may be deemed adequate to meet the requirements of many designs.

Comparison of Results With Objectives

At the time the tests were planned, it was expected that the test program might able to duplicate the connection plate fractures of the prior series of full scale connections. Some simulated details with "bad" configurations would have fractures in the connection plates near the tips of the column flanges and would exhibit less post-yield ductility. Other simulated details with "good" configurations would avoid fractures in the connection plates and would exhibit excellent post-yield ductility.

As the test program progressed, it was found that the results were not quite as clear-cut as hoped for. No fractures initiated in the connection plates at the column flange tips as occurred in the previous full-scale connection tests. Perhaps the added bending strain imposed by a moment in addition to the axial force is necessary to trigger fracture. However, it is believed that definite trends have been exhibited in the experimental program and that these trends support the recommendations which will be made for design.

The load-deflection curves of Fig. 18 and 21 are the best measure of overall performance of the specimens since they exhibit the integrated effect of everything that happens to the connections. All of the curves in both figures show two initial straight line slopes, an elastic range up to the expected yield load and then an apparent strain-hardening range at approximately the same slope thereafter. The apparent strain-hardening slope is steeper than would be calculated for a simple tensile member using coupon strain-hardening values. Unfortunately, the theoretical finite element calculations were halted when full plastification of the tension flange was reached. The calculations were conducted long before the tests and a long yield plateau was expected at that point. Since 20 to 30 complete finite element analyses were needed up that point for each curve, they were quite expensive.

In the first series of tests with the tension flange stressed perpendicular to the direction of loading, the three specimens without extended connection plates are lower in load and total elongation (A, A_{rev}, and D). (It should be noted that the deflections plotted for specimen A_{rev}. are deceivingly large because of experimental errors in mounting of the deflection gages. The deflection should probably be about the same as for specimen A.)

The specimens with extended connection plates (B, C, and E) all achieved higher loads and greater deflections than those without extended plates. Design recommendations to be presented later suggest

that specimens B and C should have had connection plates 1-3/8 inch thick to allow for shear lag, in which case they may have exhibited even better performance.

It is especially significant that specimen E shows that it is possible to have a successful connection without welding the connection plate to the column web. It was accomplished by extending the connection plate and increasing the thickness to allow for shear lag. There is a dramatic improvement shown between specimens D and E where the only difference is the extension of the connection plate.

The load-deflection curves for the second series of tests with the tension flange stressed parallel to the direction of rolling are all shown in Fig. 21. The apparent better ductilities of all of these specimens against the first series should probably be attributed to the better ductility of steel stressed parallel to the direction of loading. The only joint in the set that did not develop the full strength of the tension flange was the one without an extended connection plate (A2). All the other three (B2, C2, E2) had good ductility and developed the full plate strength.

One note of caution is necessary in comparing the ductility of these simulated details with their possible prototype connections. The free length for ductile behavior in a prototype connection probably spans only the two or three inch length over the cope hole provided in the beam web to facilitate making the groove weld of the beam flange. In the simplified detail specimen, approximately two feet of plate length is available for ductile elongation. In most of the test specimens, deflections were measured over a shorter gage length commensurate with the typical cope hole length and behavior was proportional to that measured over the full specimen length.

Comparison of the results for rectangular extended connection plates with tapered extended connection plates (B with C and B2 with C2) shows no significant differences in these four tests. Current AWS

specifications would dictate a transition in width with a 1 in 2.5 slope when the flange plate is narrower than the connection plate. The basis for this requirement is not known. It is probably necessary for fatigue situations.

The evidence of the test series here suggests that for static situations, the rectangular extension is every bit as good as the tapered extension.

6 THEORETICAL DISCUSSION AND DESIGN GUIDELINES

6.1 Theory

Connection plates which are essentially the same thickness as the flange plate they connect suffer from in-plane flexibility which promotes shear lag. The outer edges of the connection plats fastened to very stiff column flanges generate stresses at the outer edges of both connection plates and beam flanges much higher than the average stress in the plate or flange. In contrast, the end of the connection plate fastened to the column web pulls against the most flexible part of the column. The lower resistance of the web generates much smaller stresses than the average at the center of the connection plate and beam flange. The uneven distribution of stresses is the reason for shear lag and for the susceptibility to fracture at the outer edges of flanges and connection plates.

Remedial methods to help even out the stress distribution are stiffener plates on the opposite side of the column web and increases in thickness of the connection plate. Stiffener plates welded perpendicular to the column web serve as a "bridge" to help the column web resist bending perpendicular to its plane. Less deflection at the center of the column web improves but does not entirely correct the stress concentration at the edges of flange and connection plates. When a connection plate of increased thickness is provided, the stress is reduced due to the increase in gross area. The thicker plate also has increased in-plane bending stiffness to help decrease the severity of the column web bending and thus improve the stress distribution in the beam flange plate. Therefore, it can be recommended that the thickness of the connection plate be checked for both the reduced amount of shear force and for the tensile force passed to the column web. The design of the fillet welds for the connection plate should be adjusted accordingly.

6.2 Design Guidelines

Design guidelines are needed for the proportioning of connection plates to resist the shear lag effects of forces applied by tension flanges. Three cases can be identified based on how the connection plate is fastened to the column:

1. There is a backup stiffener and a connection plate, both welded to the column web and flanges.
2. There is no backup stiffener and the connection plate is welded both to the column web and flanges.
3. There is no backup stiffener and the connection plate is welded only to the column flanges.

The design thickness of the connection plate will be checked against two criteria:

1. An effective area needed to resist the tensile force applied by the beam tension flange.
2. A shear area along the two connected edges of the connection plate parallel to the line of flange force.

Shear Lag

A design approximation will be based on the shear lag recommendations of Munse and Chesson and the stress distribution patterns determined by Shen [Munse and Chesson, 1963; Shen, 1981a].

The effective area A_e of a connection plate with shear lag is

$$A_e = C_t A_g \qquad (1)$$

where

A_g = the gross cross sectional area of the connection plate t_p w

C_t = reduction factor for shear lag

$$C_t = (1 - x/L) \qquad (2)$$

where

x = lateral distance from centroid of force to the line of fasteners

L = length of the shear path

With welded connection plates, it will be assumed that the beam flange tensile force is divided in half and the resultant of each half is centered at a distance w/4 away from the line of welds. Thus $x = w/4$, or approximately $x = d_c/4$

where

d_c = depth of column

w = width of connection plate

t_p = thickness of connection plate

When the connection plate is welded only to the column flanges, the length L of the shear path on each flange is approximately $b_c/2$. Therefore, the reduction factor for a connection plate welded only to the column flanges is:

$$C_t = 1 - (d_c/4)/(b_c/2)$$

$$C_t = 1 - d_c/(2\ b_c) \qquad (3)$$

When the connection plate is welded to both the column flanges and the column web, and a backup stiffener is provided as well, the length of the shear path is approximately the column flange width b_c. Then the reduction factor for a connection plate fully welded and with a backup stiffener is:

$$C_t = 1 - (d_c/4)/b_c$$

$$C_t = 1 - d_c/(4\ b_c) \qquad (4)$$

Another consideration for the fully-welded connection plate with a backup stiffener is that not all of the force in the connection plate needs to be transmitted as shear on the column flange welds.

The finite element studies of Shen show that less than 60 percent of the beam flange load is transmitted from the connection plate to the column flanges in a stiffened connection [Shen, 1981a].

Once the shear lag reduction factor is determined from either Eq. (3) or (4), it can be substituted into Eq. (1) and used to determine the amount of gross area A_g needed to provide the required effective area A_e to resist the beam flange force. The gross area of the connection plate will be

$$A_g = w\ t_p \tag{5}$$

where

$w = d_c - 2\ t_c$

t_p = required thickness of connection plate

Shear Area

In addition to determining the connection plate thickness based on the effective area needed to allow for shear lag, the shear area of the connection plate should be checked.

The shear area A_s provided by the connection plate is

$$A_s = 2\ L\ t_p \tag{6}$$

where

L = length of each shear path

$= (b_c/2) - k_1$

k_1 = distance from y-y axis of column to tangent of fillet on column flange

The shear capacity of the connection plate must equal 100 percent of the beam flange force when the connection plate is welded only to the column flanges. If shear yield stress τ_y is assumed to equal $\sigma_y/\sqrt{3}$ then

$$A_s = \sqrt{3}\, A_f \tag{7}$$

From Eq. (6) and (7), the connection plate must equal or exceed t_p from Eq. (8) when the connection plate is welded only to the column flanges.

$$t_p = \sqrt{3}\, A_f/(2\ L) \tag{8}$$

Shen has shown that when the connection plate is welded to the column web as well as the column flanges, part of the force is carried to the web of the column through tension in the end of the connection plate. The reduction in shear force may permit a reduction in the connection plate thickness, provided adequate effective area is present based on Eq. (1).

When the connection plate is welded to the column web and flanges, but no stiffener is present, less than 80 percent of the beam flange force is transmitted to the column flange through shear. On this basis, the required thickness of connection plate could be 80 percent of t_p from Eq. (8).

$$t_{ps} = 0.8\sqrt{3}\, A_f/(2\ L) \tag{9}$$

Since the effective area in this case also is required to carry only 80 percent of the beam flange force, the value of t_p from Eq. (5) can be reduced to 80 percent.

$$t_p = 0.8\ A_e/(w\ C_t) \tag{10}$$

The connection plate thickness should be based on the larger value from Eq. (9) or (10).

When a connection plate is welded to both column web and flanges, and is backed up by a stiffener welded on the opposite side of the

column, less than 60 percent of the beam flange force is carried by shear on the connection plate according to Shen [Shen, 1981a]. The remaining 40 percent passes in tension to the column web. Shear forces on the stiffener finally transfer the remaining force to the far half of the column flange.

The effective area calculation of Eq. (4) accounts for the doubled shear path. The connection plate thickness based on shear stress should also be checked against the amount required by 60 percent of t_p from Eq. (8).

$$t_{ps} = 0.6\sqrt{3}\, A_f/(2\, L) \qquad (11)$$

The connection plate thickness should be based on the larger value from Eq. (5) or (11).

Connection Plate Extension

By extension of the connection plate length, the groove weld connecting the beam flange to the connection plate can be placed far enough outside the plane of the column flange tips to reduce the triaxial stress effects. Shen's parametric studies indicated a beneficial stress distribution resulting from extension of the connection plate.[Shen, 1981a] The test results reported here showed a definite improvement in the toughness after yielding of specimens with either a tapered or rectangular extension of 2.7 or 3.0 times the beam flange thickness, as compared with specimens having no extension. Where the connection plate projected one beam flange thickness or less (a minimum amount to allow placing a groove weld) the specimens showed a tendency to crack near the groove weld and had less toughness after yielding. A second measure of the extension length provided in the tests was the extension-to-connection-plate-width ratio. This ratio was 0.24 in all the applicable specimens in the test series. For an initial design recomendation, the extension length will be recommended as a multiple of beam flange thickness.

For design, it is recommended that the flange connection plate, either rectangular or tapered, be extended past the column flange tips by an amount equal to or greater than three times the beam flange thickness. It should be noted that AWS recommends that either the plate or the groove welds be tapered to allow for transition in thickness when a flange is butt-welded to a connection plate of substantially greater thickness.

Distribution of Forces to Welds

In the development of Eq. (7) through (11) it was shown that, depending on the welding and stiffening details, 100, 80, or 60 percent of the beam flange force could be assumed to be carried by shear on welds between the connection plate and column flanges. The remaining 0, 20, or 40 percent would be transmitted to the column web on welds connecting the end of the connection plate. To design the welds, any line of weld will be assumed to be stressed uniformly on the throat of the weld. The size of any weld will be based on its share of the total force and a length of weld which assumes that the weld is stopped as it reaches the tangent point of the curved fillets at the intersection of the column flange and web. The corners of the connection plate would be clipped to allow the plate to fit between the flanges of the column and against the web of the column.

The ideas expressed above were used to construct Table 5 which gives guidance for assigning forces to four different weld types a, b, c, and d for three different connection plate welding and stiffening cases. The welds a, b, c, and d are shown in Fig. 10.

6.3 Design Example

The connections simulated by the detail specimens of this study required the flange of a W 27 x 94 beam to be connected to a W 14 x 257 column. Selected data about the members will be tabulated and the results of applying the design formulas developed above will be listed for the alternate connection designs.

Given Data:

Beam flange: $A_f = 10 \times 1$

Column:
$d_c = 16.38$
$b_c = 15.995$
$t_c = 1.89$
$k_1 = 1.1875$
$k = 2.5625$

Eq. (3) gave a reduction factor C_t of 0.488 for a connection plate welded only to the column flanges. Eq. (4) gave a C_t of 0.743 for a connection plate welded to the column web and flanges.

Connection plate thicknesses required for the three cases of welding and stiffening may be based on effective area to allow for shear lag or on the edge shear force. Plate thickness values rounded up to the nearest plate thickness provided by usual mill practice are given below along with the equation numbers involved in the calculation.

Case	Equation No.	Basis	Required Plate Thickness
(1)	(4) & (5)	Effective Area	1-1/8
	(11)	Shear Force	13/16
(2)	(10)	Effective Area	1-1/8
	(9)	Shear Force	1-3/8
(3)	(3) & (5)	Effective Area	1-5/8
	(8)	Shear Force	1-3/8

In all these cases, the plate thickness was controlled by the shear lag effective area.

Selection of weld sizes may be based on Table 5. For the same design cases listed above, the substitution of numeric values results in the fillet weld sizes tabulated below. It should be noted how much less welding is nedded between the column web and the connection plate or back-up stiffener when allowance is made for the force the column web can actually resist. In the test specimens, a constant fillet

weld size of 3/4 in was used throughout, with no signs of distress. The material was E70xx as used in the examples. The equations in Table 5 would be usable either with allowable stress flange forces and allowable weld shear stresses or with plastic design flange forces combined with plastic design weld stresses.

Weld Design Table

$P = 500$ k $d_c = 16.38$ $b_c = 15.995$ $k_1 = 1.825$

Case	Weld Location	No. of Welds	Force in Each Weld	Length of Each Weld	Force/ Length	E70xx Weld Size
(1)	a	4	75	6.12	12.25	9/16
	b	2	100	11.25	8.88	3/8
	c	2	100	11.25	8.88	3/8
	d	4	50	6.12	8.17	3/8
(2)	a	4	100	6.12	16.33	11/16
	b	2	50	11.25	4.44	3/16
(3)	a	4	125	6.12	20.41	7/8

7 SUMMARY

The following conclusions can be drawn from the results of this theoretical and experimental program:

- All ten simulated detail tests reached an average tensile stress equal to or greater than the coupon yield stress of the flange material.

- There was a definite difference in the post-yield capacity of specimens having the connection plate extended so the groove weld was removed from the region of the column flange tips. All of the details with extended connection plates showed better performance than those with the groove weld at the region of the column flange tips.

- The rectangular extended connection plates appeared to be equal in performance to the tapered extended connection plates. Specimens of both types exhibited extra deformation capacity after reaching the yield load.

- Four specimens (E, B2, C2, E2) fractured in the flange plate 10 or more inches outside the groove weld. The connections thus developed the full strength of the member joined.

- Two specimens with backup stiffeners and extended connection plates (B2, C2) developed the full strength of the member despite having no increase in the connection plate thickness.

- A specimen not welded to the column web and with a thick connection plate and tapered extension (E) developed the full strength of the flange plate.

- A specimen with a thick connection plate not welded to the column web, but with no extension of the connection plate (D) fractured at the lowest load of all specimens.

Based on the theoretical and experimental results, design recommendations for tension flange connections of weak axis moment connections are presented. Recommendations cover the following aspects of the connection design:

- Thickness of the connection plate based on effective area to resist shear lag.

- Thickness of the connection plate based on shear forces to be transmitted to the column flanges.

- Length of extension of the connection plate to alleviate triaxial stress conditions in the vicinity of butt welds.

- Recommended proportions of the beam flange force to be allowed for in the design of fillet welds:

    * between the sides of the connection plate and the column flanges.

    * between the end of the connection plate and the column web.

    * between the column web and the end of the back up stiffener.

    * between the edges of the back up stiffener and the column flanges.

The design recommendations for connection plates and welds recognizes that the design may choose to treat the connection plate in any one of three configurations each of which requires different connection plate thicknesses and fillet weld sizes:

- the connection plate is welded to both the column flanges and column web and a backup stiffener is provided.

- the connection plate is welded to the column flanges and web but no backup stiffener is provided.

- the connection plate is welded to the column flanges but not to the column web.

The findings of the investigation showed that connections with rectangular extended connection plates are just as suitable as those with tapered extended plates. Implementation of this finding as a design recommendation would conflict with AWS Welding Code requirements for transitions in plate width. It would appear that a compromise might be necessary here.

It is recommended that a limited series of full-scale beam-to-column connections be designed by the recommendations presented here and tested both statically and with reversed repeated loading in order to confirm the suitability of the connections for static and

earthquake design.

8 ACKNOWLEDGEMENTS

This work was conducted at Lehigh University in the Fritz Engineering Laboratory, of which Dr. Lynn S. Beedle is director.

The results reported herein form part of the investigations "Fracture of Moment Connections" sponsored by the American Iron and Steel Institute (Project No. 317) and American Institute of Steel Construction, and "Fracture of Steel Moment Connections Due to Seismic Building Loadings", sponsored by the National Science Foundation (Grant No. CEE-8022041). We wish to thank Mr. Albert C. Kuentz, Mr. Walter Fleischer, Mr. William A. Milek, Jr., and Dr. Michael P. Gaus for their assistance in obtaining funding for this research.

Prior tests were carried out in a research program on beam-to-column connections sponsored jointly by the American Iron and Steel Institute, American Institute of Steel Construction, and the Welding Research Council. The research was carried out under the guidance of the WRC Task Group on Beam-to-Column Connections of which Mr. John A. Gilligan is chairman. The interest, encouragement, and guidance of this committee is greatefully acknowledged.

Mr. Xianru Wang was sponsored as a Visiting Research Engineer at Lehigh University by the government of the People's Republic of China from November 1981 to December 1982. During this period Mr. Wang was on leave from his position as Research Engineer with the Institute of Hydraulic Research, Yellow River Conservancy Commission, Zhengzhou, Henan Province, the People's Republic of China.

Many helpful suggestions in the preparation of this report were provided by Dr. Le-Wu Lu and by Dr. Beedle. Advice on fracture was provided by Dr. John W. Fisher, Dr. Alan W. Pense, and Dr. Richard Roberts. Dr. Bruce R. Somers provided advice on fracture tests and performed the fractography.

Mr. John H. Brooks, Jr. of Neal S. Moreton and Associates

performed the ultrasonic tests of welds.

The authors wish to extend their thanks to those who helped in preparation of specimens and test setups and in the actual testing, especially Messrs. Roger G. Slutter, Hugh T. Sutherland, Robert R. Dales, Charles F. Hittinger, Raymond Kromer, Russell Longenbach, and Shiunn-Jang Wang. Mr. Richard N. Sopko took all test photographs and prepared the resulting prints and slides.

The assistance of Mr. Jack Gera in preparation of drawings is appreciated.

The report was prepared using the Scribe Document Production System on the facilities of the Lehigh University Computing Center.

9 TABLES

Table 1: LIST OF TEST NUMBERS

Test Number	Specimen Identification	Simulated Beam Flange Size (in x in)
469-T1	A	10 x 1
469-T2	A_{rev}	10 x 1
469-T3	B	10 x 1
469-T4	C	10 x 1
469-T5	D	10 x 1
469-T6	E	10 x 1
469-T7	A2	9 x 1-1/8
469-T8	B2	9 x 1-1/8
469-T9	E2	9 x 1-1/8
469-T10	C2	9 x 1-1/8

Table 2: DETAILS OF TESTED SPECIMENS

Specimen No.	Connection Plate Thickness (in)	Fracture Load (kips)	Fracture Load Ratio P_u/P_y	Ductility Ratio	Specimen Sketch and Fracture Trace
A	1	730	1.38	6.3	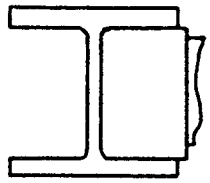
A_r	1	730	1.38	*	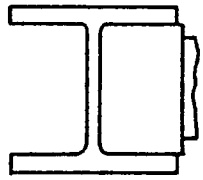
B	1	824	1.55	5.3	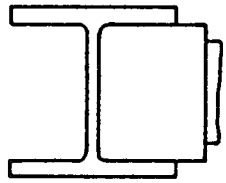
C	1	756	1.43	5.42	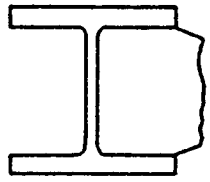
D	1-5/8	590	1.11	1.71	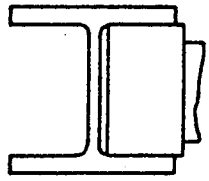
E	1-5/8	802	1.51	6.81	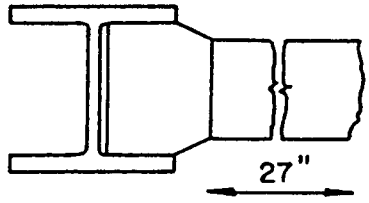

* Malfunction of deflection gage

Table 2, continued:
DETAILS OF TESTED SPECIMENS

Specimen No.	Connection Plate Thickness (in)	Fracture Load (kips)	Fracture Load Ratio P_u/P_y	Ductility Ratio	Specimen Sketch and Fracture Trace
A2	1	762	1.40	17.7	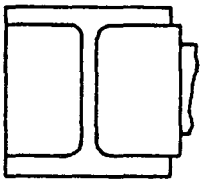
B2	1	795	1.46	16.5	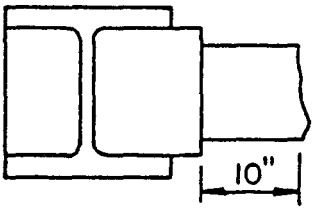
E2	1-5/8	814	1.49	*	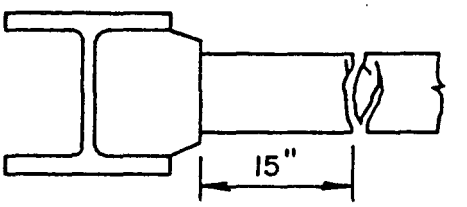
C2	1	813	1.49	29.6	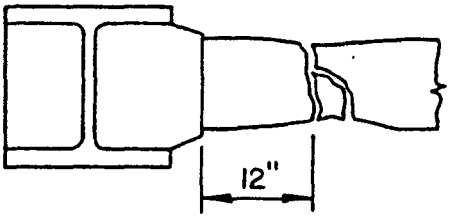

* Deflection gage malfunction

Table 3: TENSILE PROPERTIES OF THE TESTED MATERIAL

Test No.	Specimen No.	Cross-Section (in x in)	σ_y Dynamic (ksi)	σ_y Static (ksi)	σ_u (ksi)	E_{st} (ksi)
1	469-60-1	1.00 x 1.50	55.2	52.7	83.6	722
2	469-77-1	1.00 x 1.50	55.3	53.3	83.6	809
3	469-77-2	1.01 x 1.50	56.3	53.6	83.6	691
4	469-60-R1*	1.16 x 1.50	56.1	54.3	82.1	725
5	469-60-R2*	1.11 x 1.50	56.6	54.6	81.9	641
6	469-35-1-1	1.64 x 1.50	68.0	60.7	97.6	915
7	469-35-2-1	1.64 x 1.50	66.9	62.0	97.4	851

Rn*--coupons pulled in direction of rolling

Test No.	% Reduction of Area	% Elongation Max. Load	% Elongation Fracture
1	55.9	10.5	24.7
2	57.8	10.7	23.9
3	53.4	--	24.7
4	61.7	8.1	24.4
5	61.4	9.1	25.1
6	43.4	9.9	20.6
7	43.8	10.3	20.5

Table 4: LOCATION AND NUMBER OF ROSETTES AND CANTILEVERS USED IN EACH TEST

Specimen No.	Locations of Deflection Gages	Locations of Strain Gages	Sketch of Specimen
A	d	C6,D2,E2 C'2	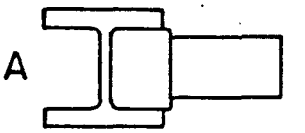
A_{rev}	d	A4,C2,D2,E2 A'2	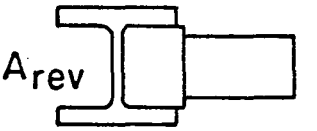
B	d	A3,C2,D2,E2 A'3	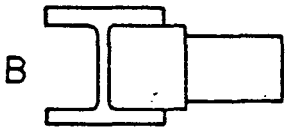
C	a,b	A4,C2,D2,E2 A'2	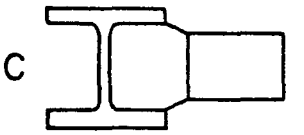
D	a,b	A4,C2,D2,E2 A'2,C'2,D'2	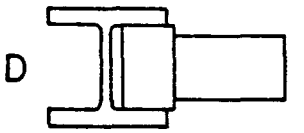
E	a,b	A4,C2,D2,E2 A'2,C'2,D'2	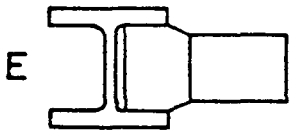
A2	a,b,c	A2,C4,D2,E2,F2 G2 A'2	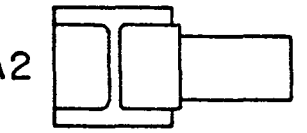
B2	a,b,c	A2,C4,D2,E2,F2 G2 A'2	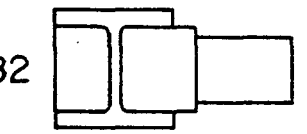
E2	a,b,c	A4,C2,D2 A'2	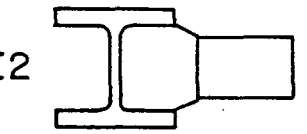
C2	a,b,c	B4,C2,D2,F2,G2 B'2	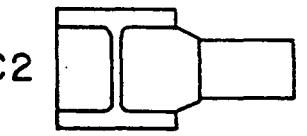

a,b,c,etc--Refers to Fig. 17
A2,C4,etc--Refers to Fig. 15

Table 5: DESIGN FORCES AND LENGTHS OF WELDS

[P = Design Value of Beam Flange Force]

Case	Weld Location	No. of Welds	Force in Each Weld	Length of Each Weld
(1)	a	4	0.6 P/4	$b_c/2 - k_1$
	b	2	0.4 P/2	$d_c - 2k$
	c	2	0.4 P/2	$d_c - 2k$
	d	4	0.4 P/4	$b_c/2 - k_1$
(2)	a	4	0.8 P/4	$b_c/2 - k_1$
	b	2	0.2 P/2	$d_c - 2k$
(3)	a	4	P/4	$b_c/2 - k_1$

Three Cases of Connection Plate Welding

(1) Connection Plate Fillet Welded to Both Column Flanges and Column Web. Fully Welded Back-up Stiffener.

(2) Connection Plate Fillet Welded to Both Column Flanges and Column Web. No Stiffener.

(3) Connection Plate Fillet Welded Only to Column Flanges.

Four Locations of Fillet Weld

(a) Fillet Weld of Connection Plate to Column Flanges. (4 Welds/Plate)

(b) Fillet Weld of Connection Plate to Column Web. (2 Welds/Plate)

(c) Fillet Weld of Back-up Stiffener to Column Web. (2 Welds/Plate)

(d) Fillet Weld of Back-up Stiffener to Column Flanges. (4 Welds/Plate)

10 FIGURES

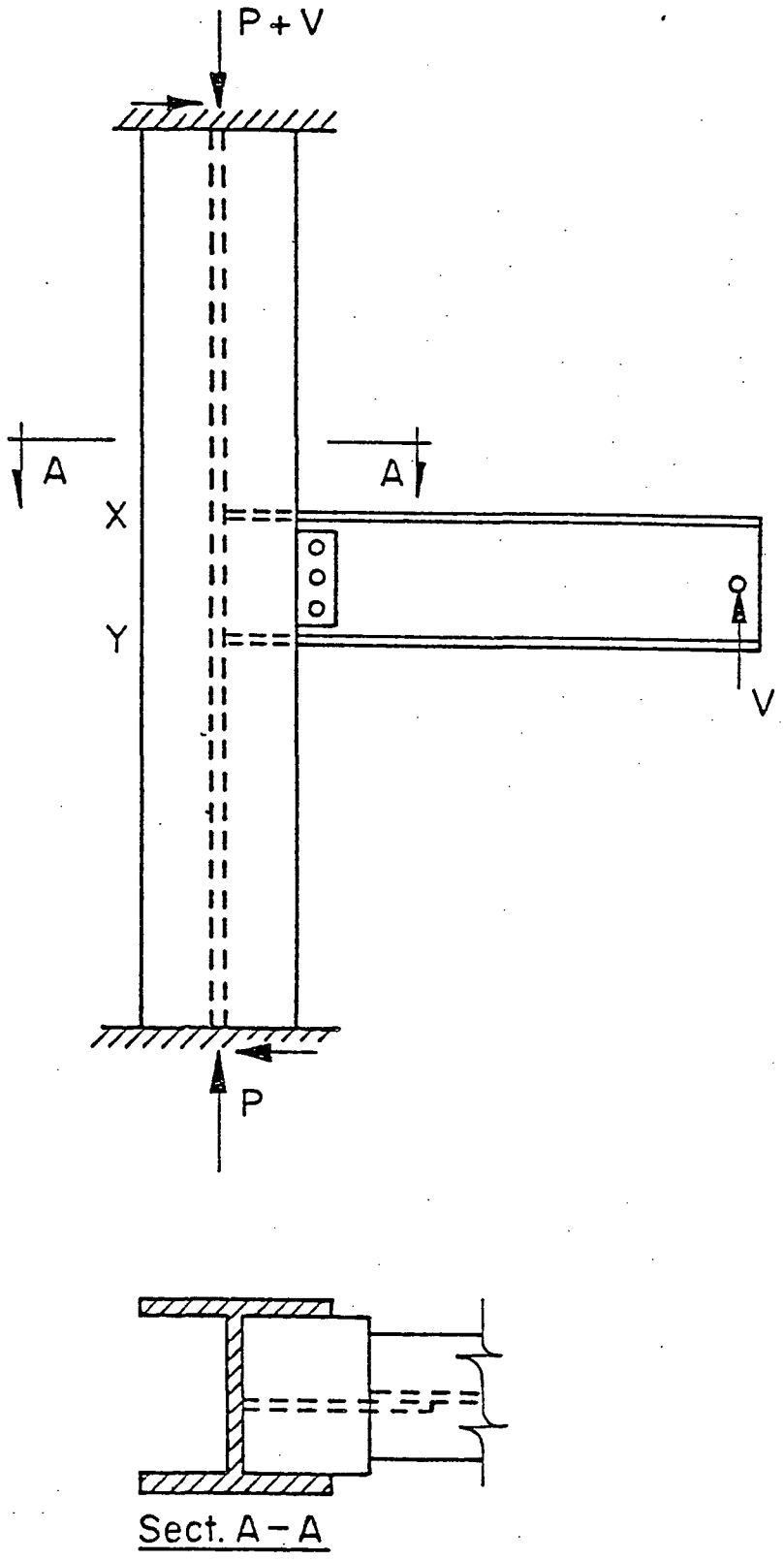

Figure 1: Typical Connection Test Setup [Rentschler, 1980]

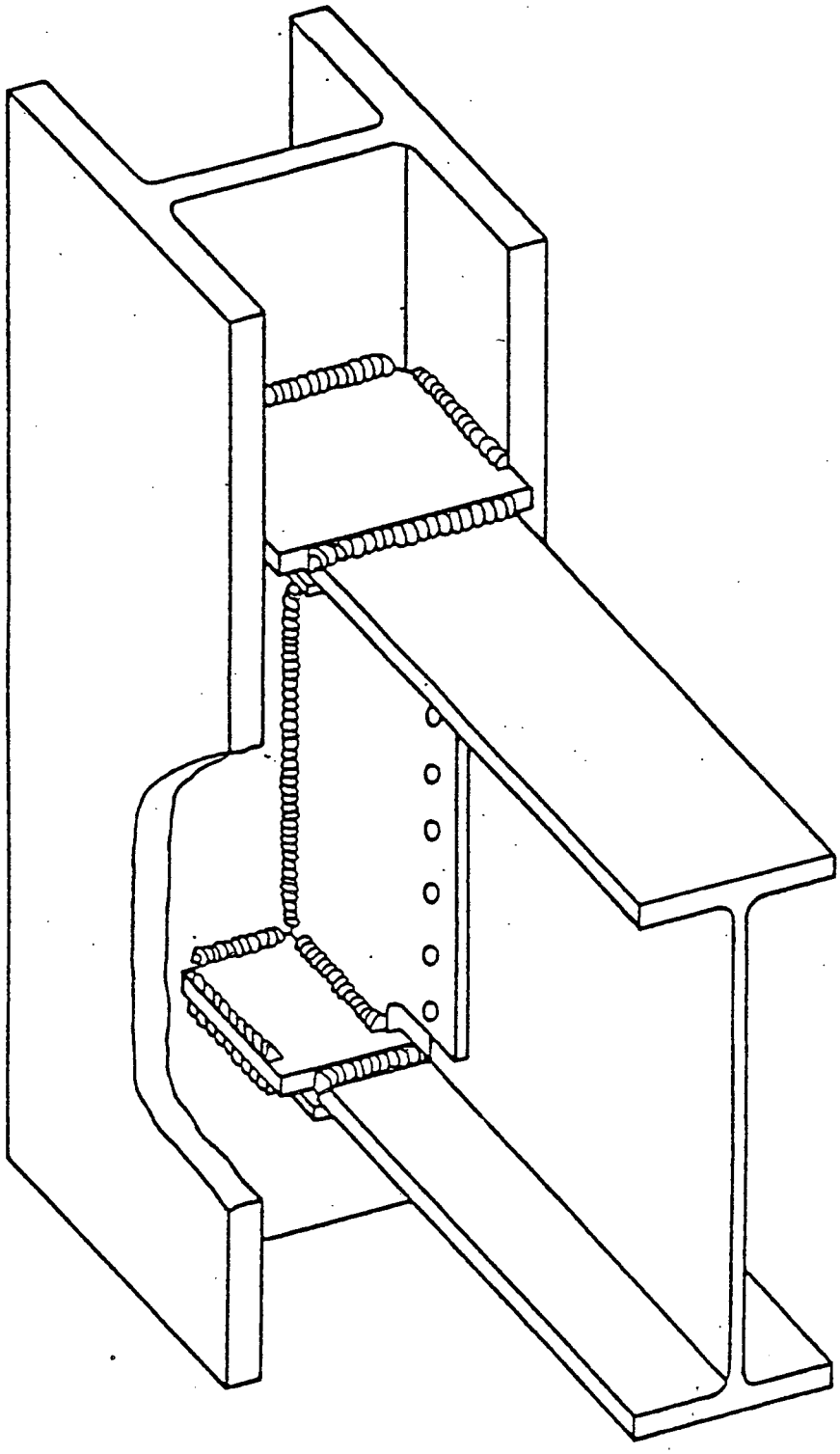

Figure 2: Typical Full-Scale Connection

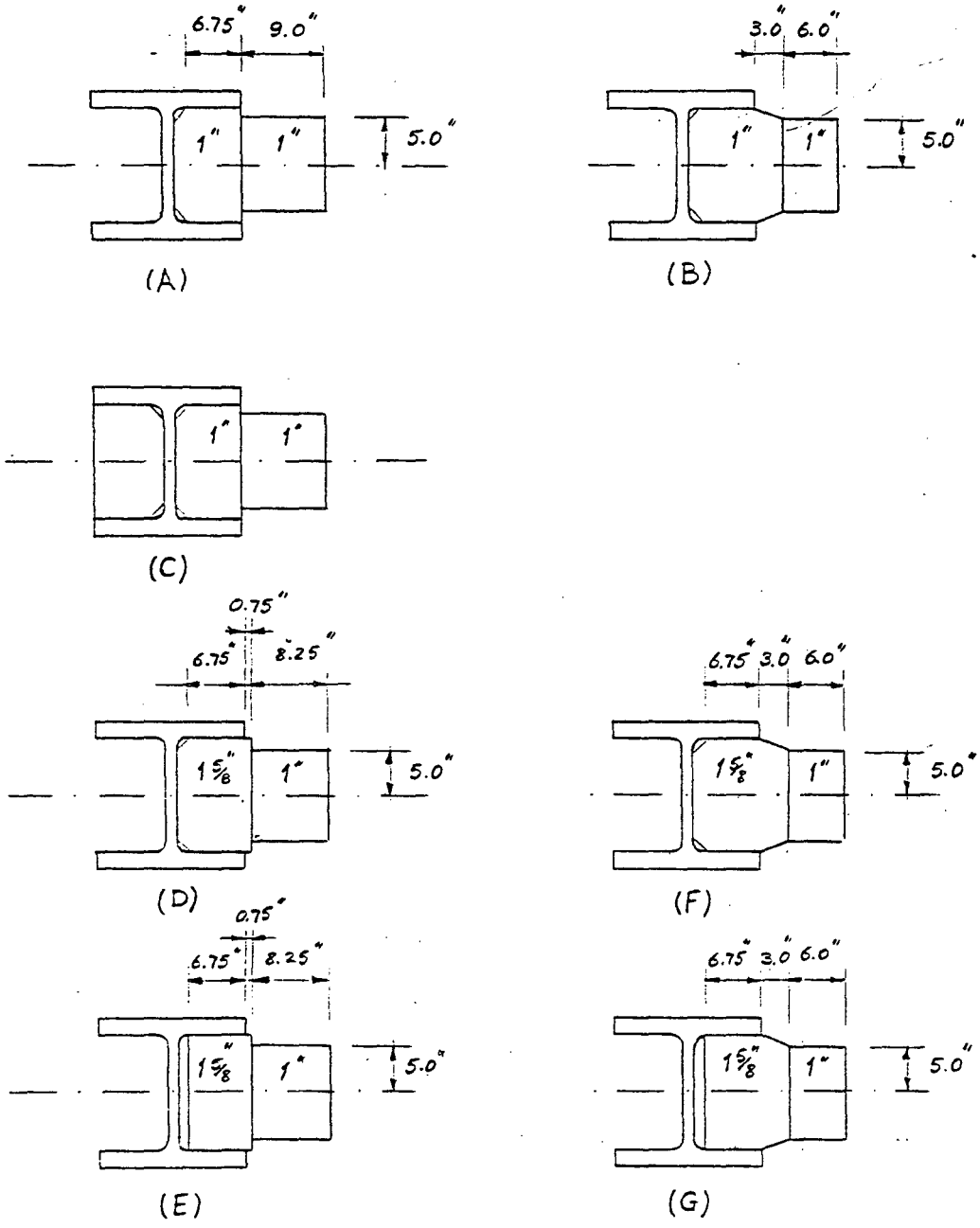

Figure 3: Dimensions of Connection Details Analyzed

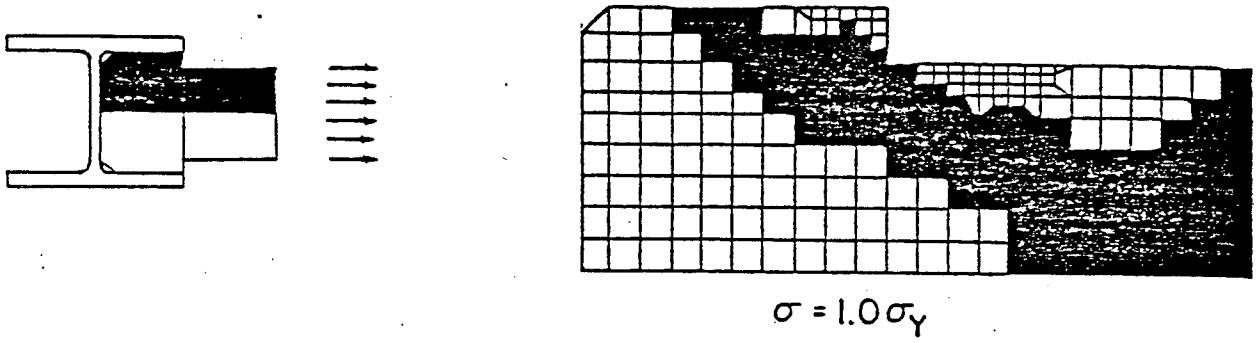

(a) Connection plate 1 in thick--welded to column web

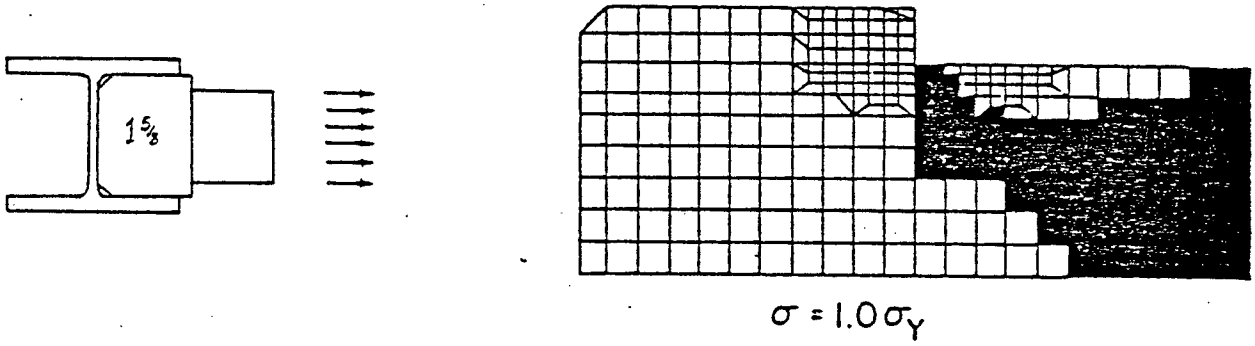

(b) Connection plate 1-5/8 in thick--welded to column web

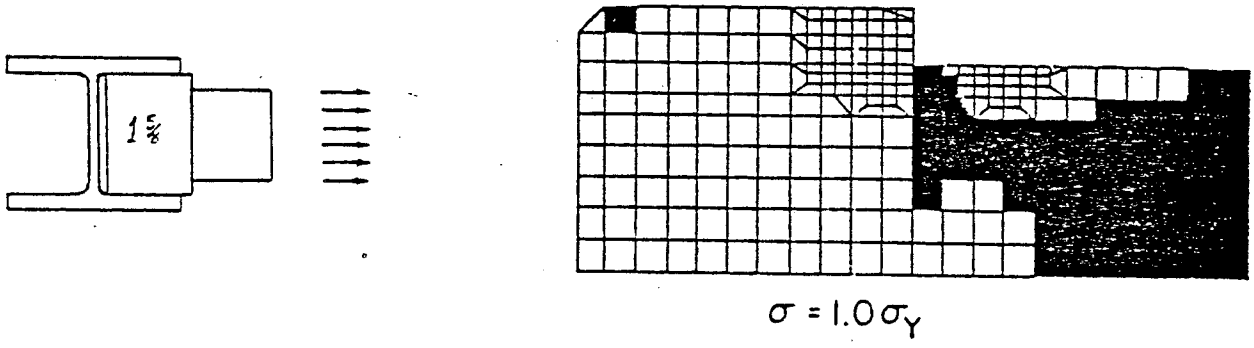

(c) Connection plate 1-5/8 in thick--not welded to column web

Figure 4: Predicted Yield Patterns of Different Details

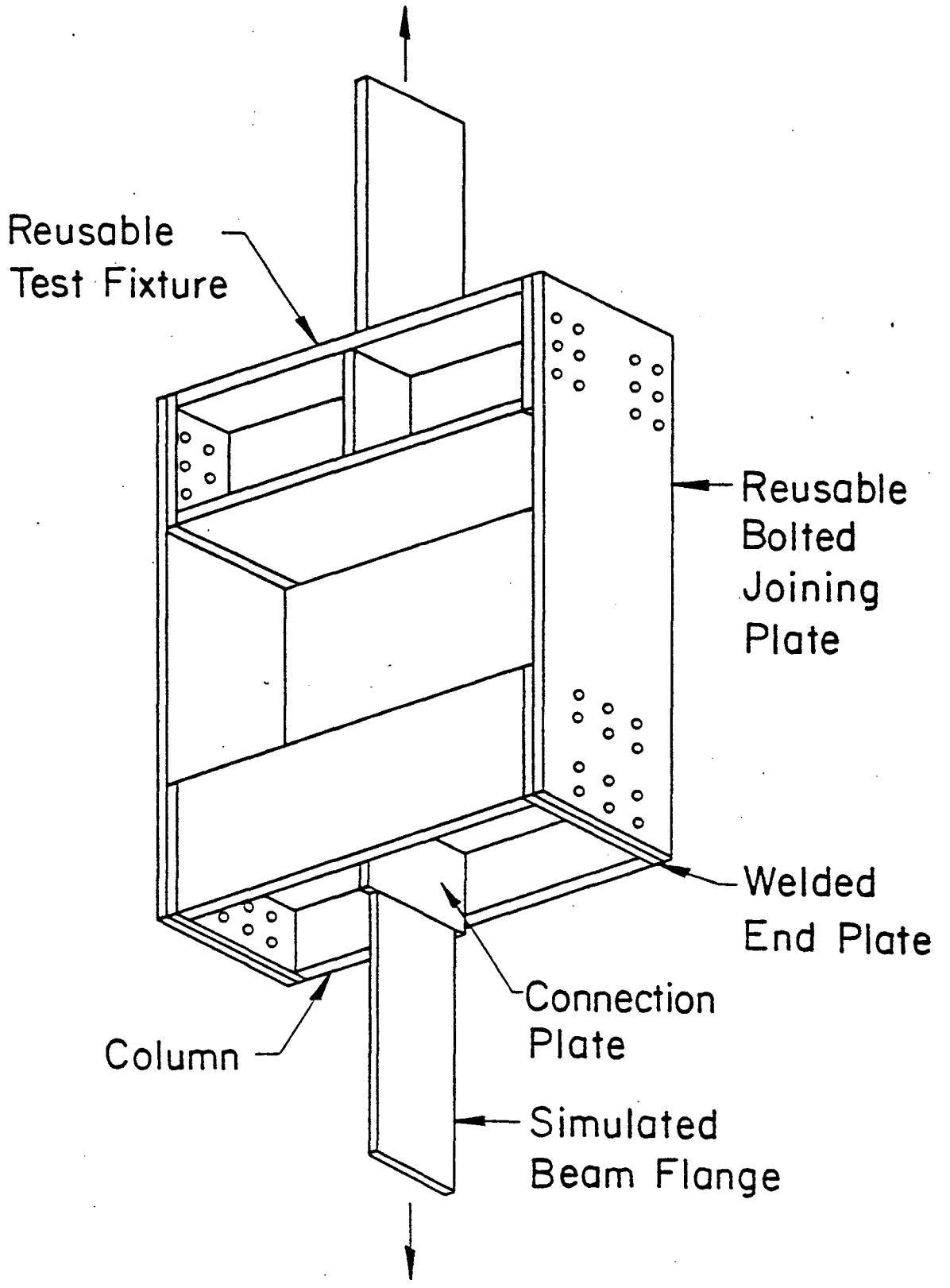

Figure 5: Test Setup

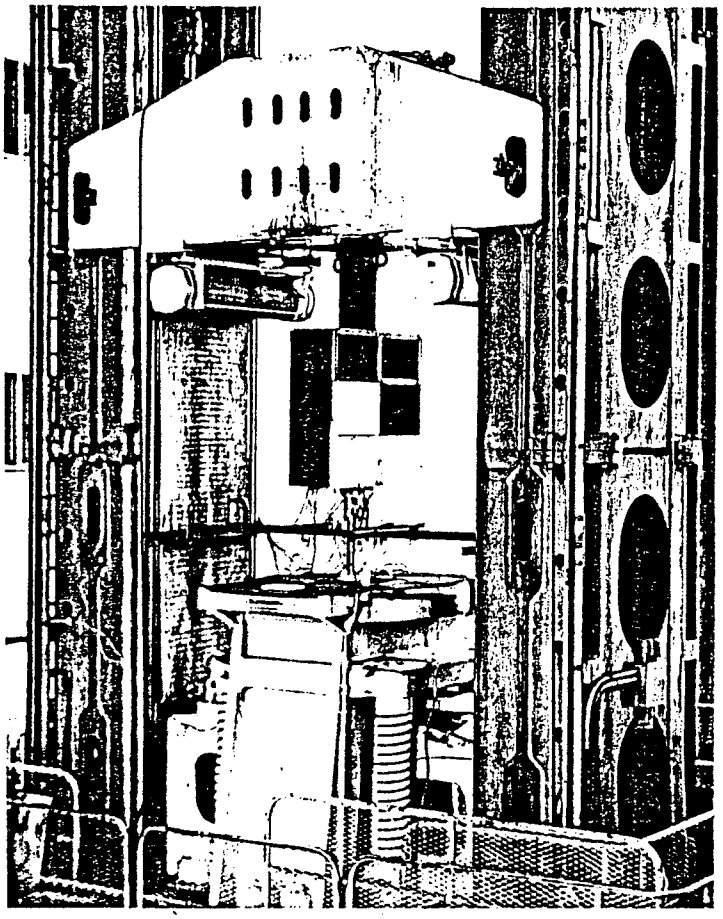

Figure 6: Specimen in the Testing Machine

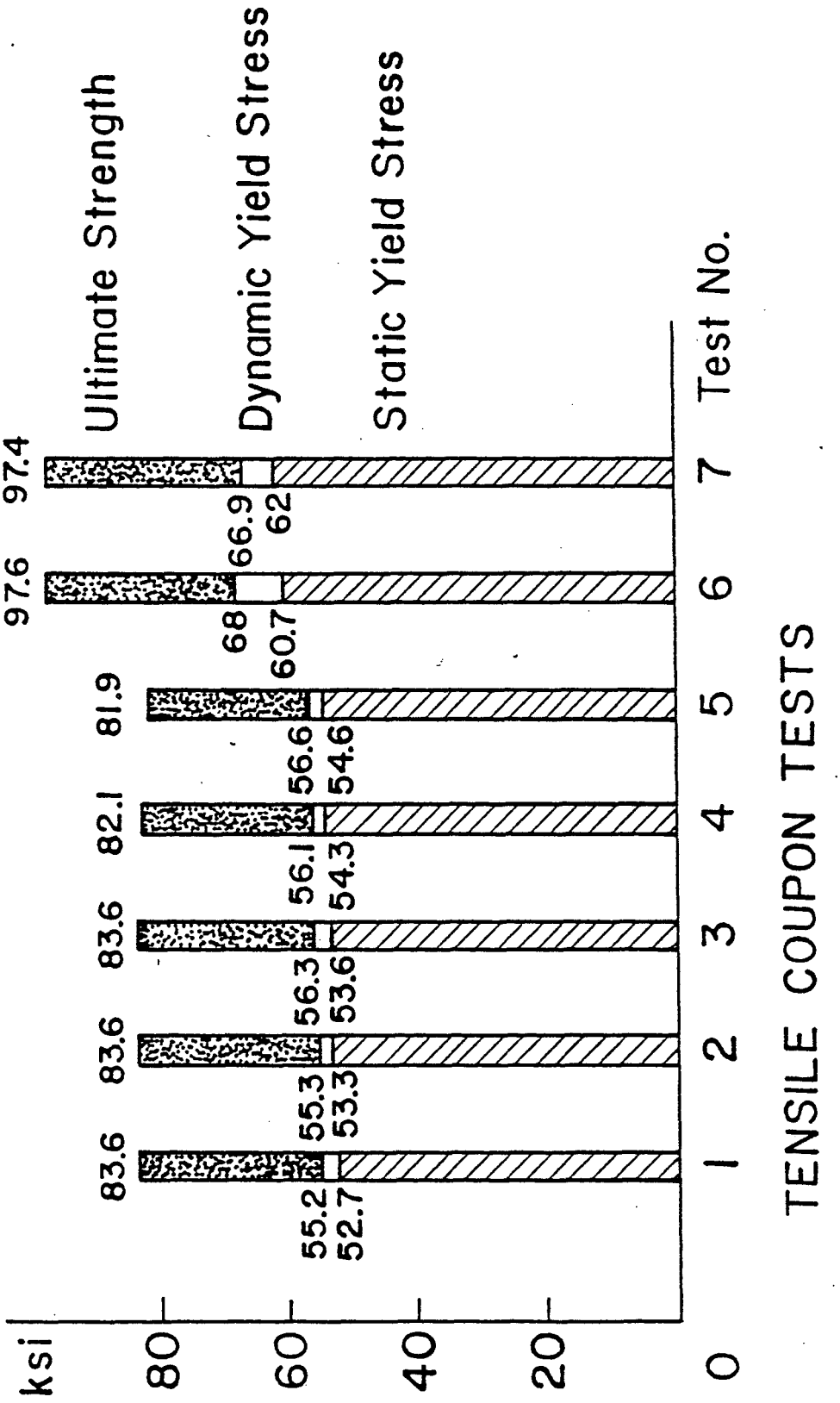

Figure 7: Yield Stresses and Tensile Strengths of Tested Coupons

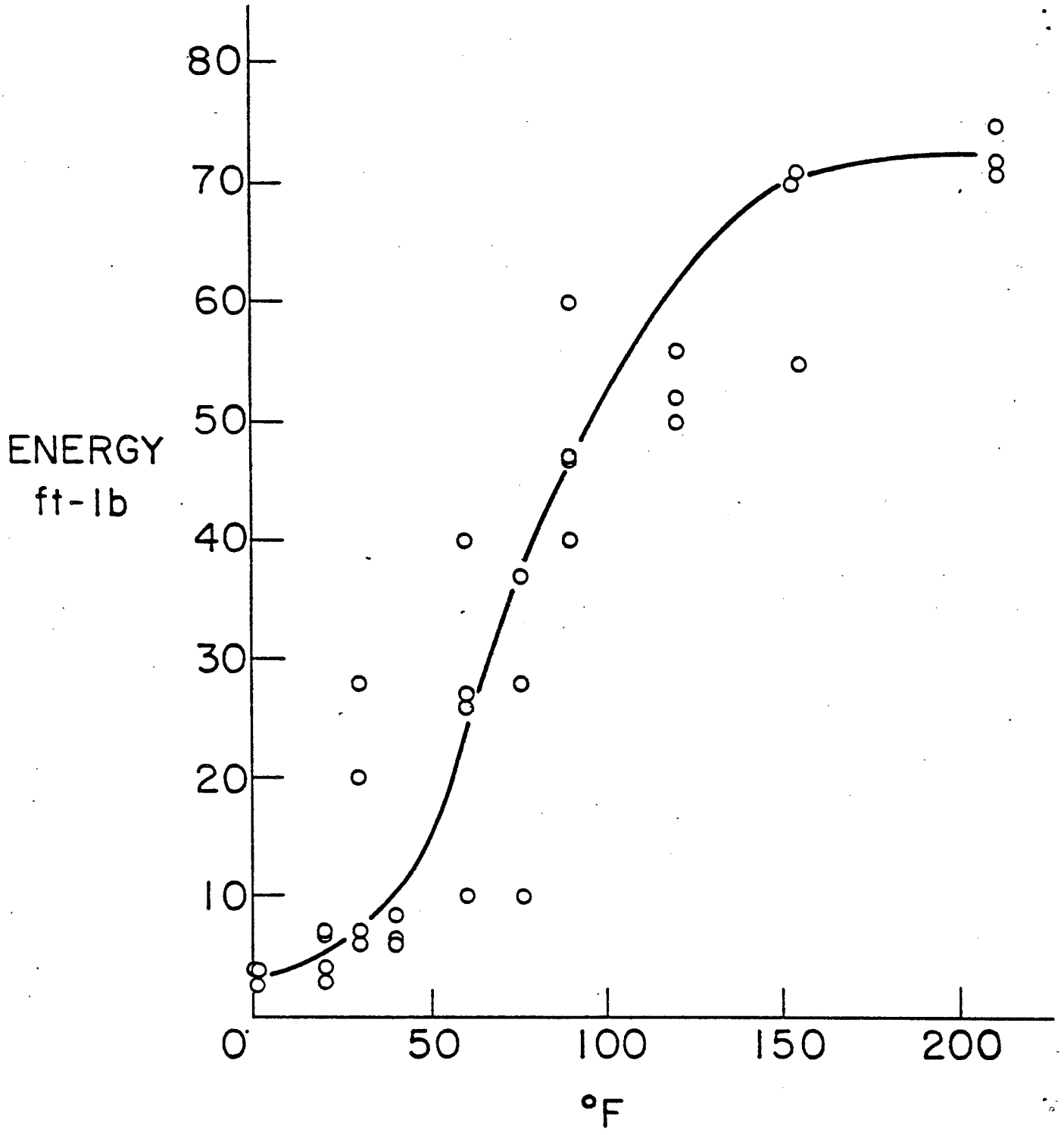

Figure 8: Charpy Impact Energy of the First Test Series

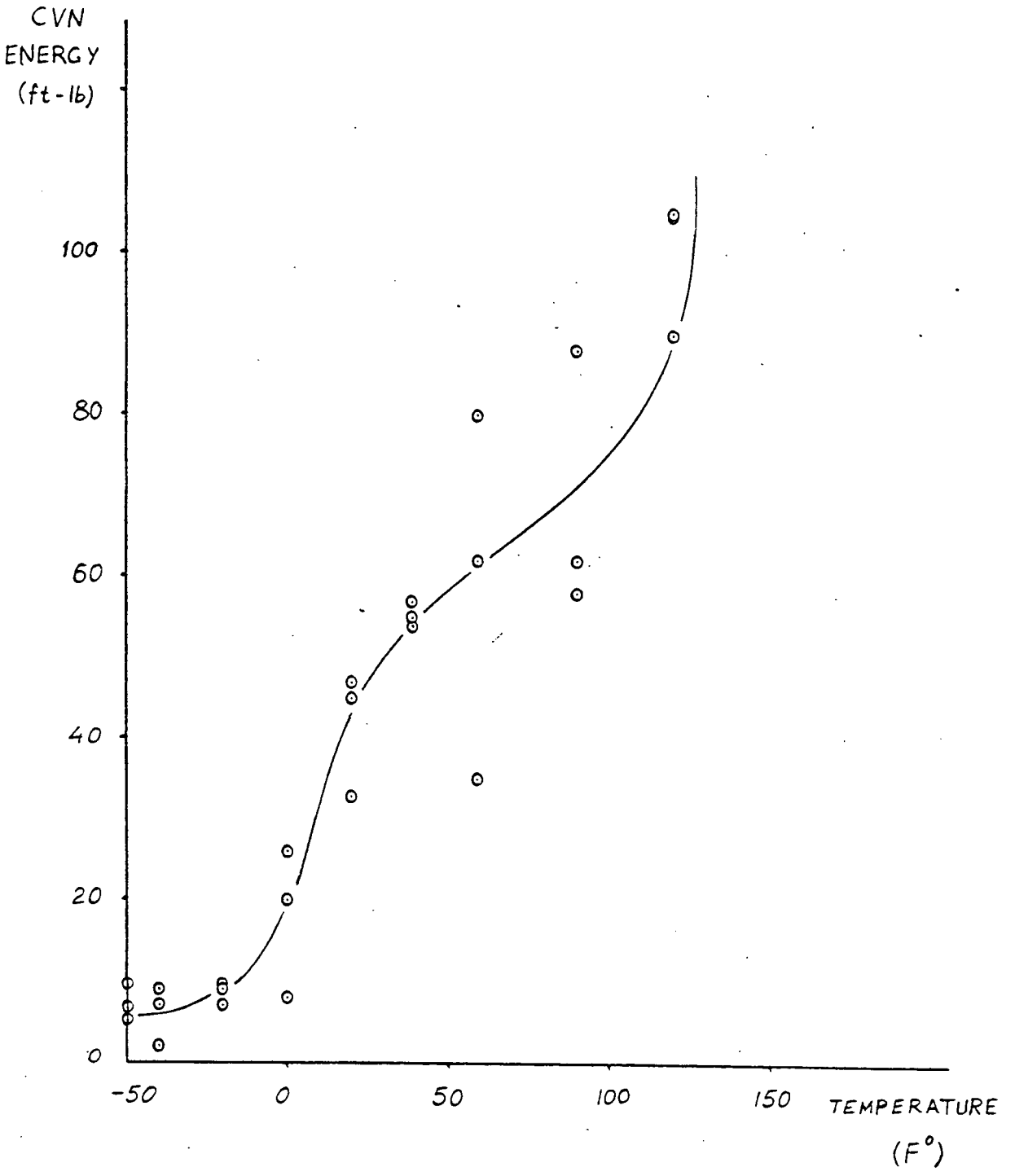

Figure 9: Charpy Impact Energy of the Second Test Series

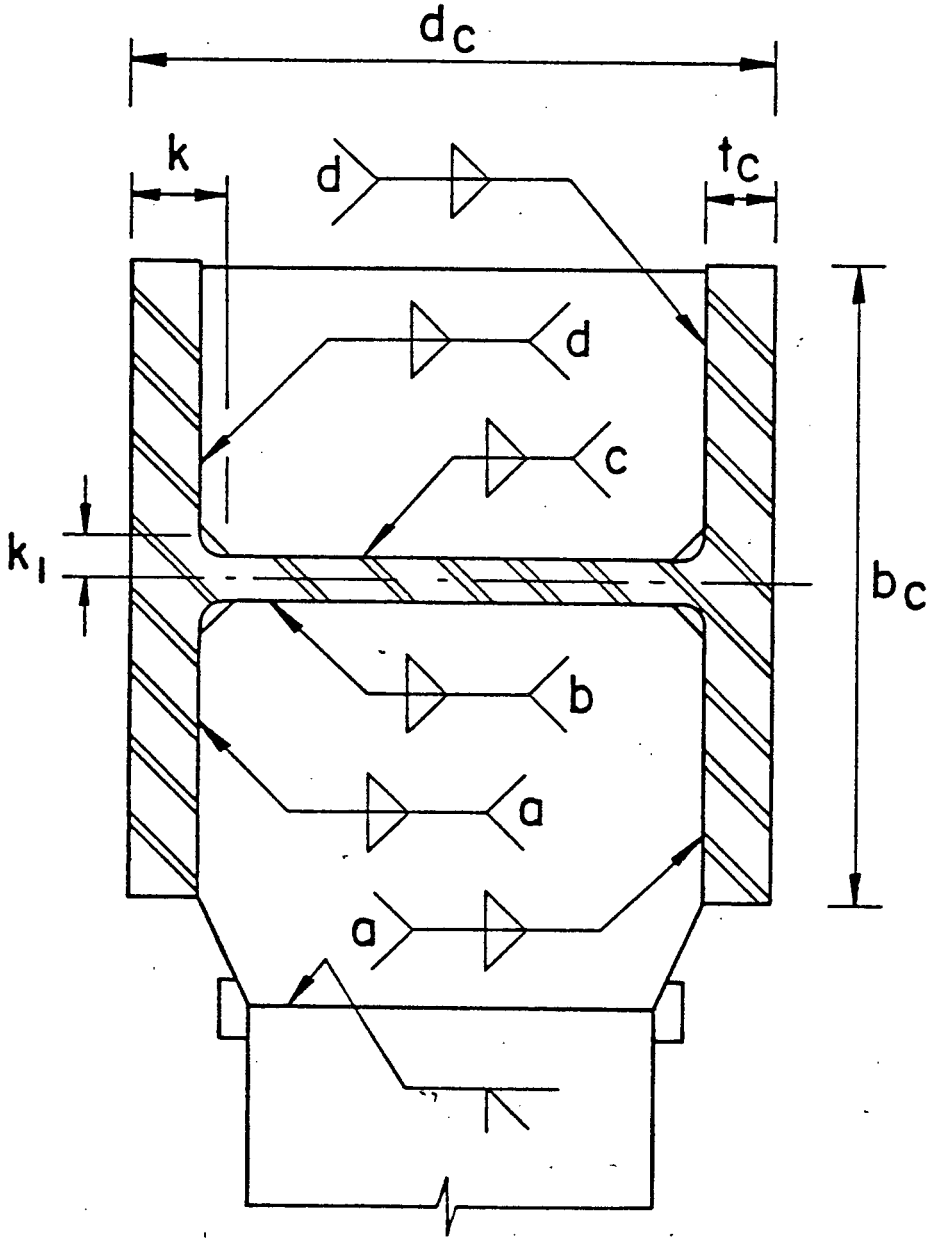

Figure 10: Design of Fillet Welds

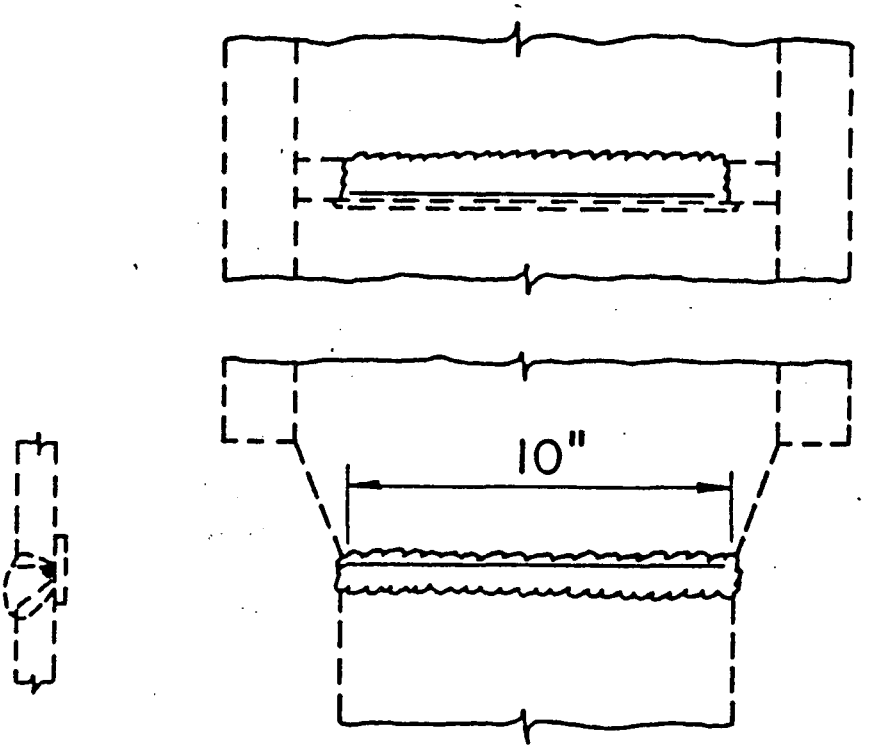

Specimen C

Figure 11: Sizes and Locations of the Groove Weld Defects in Test T4 (C)

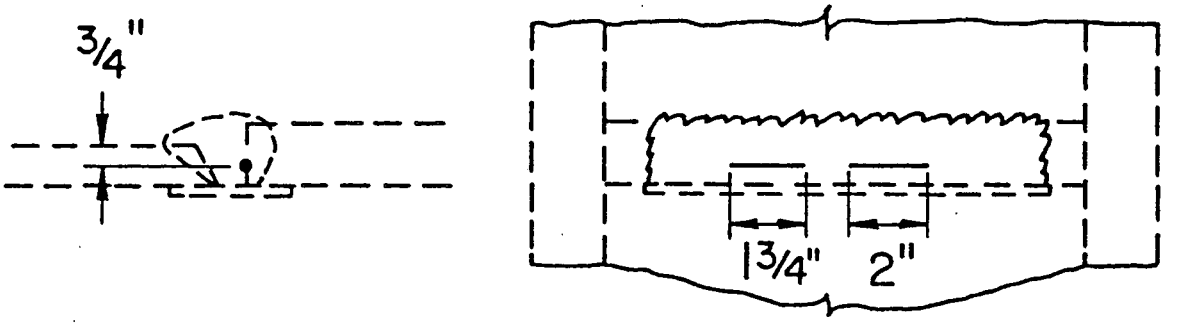

Specimen D

Figure 12: Sizes and Locations of the Groove Weld Defects in Test T5 (D)

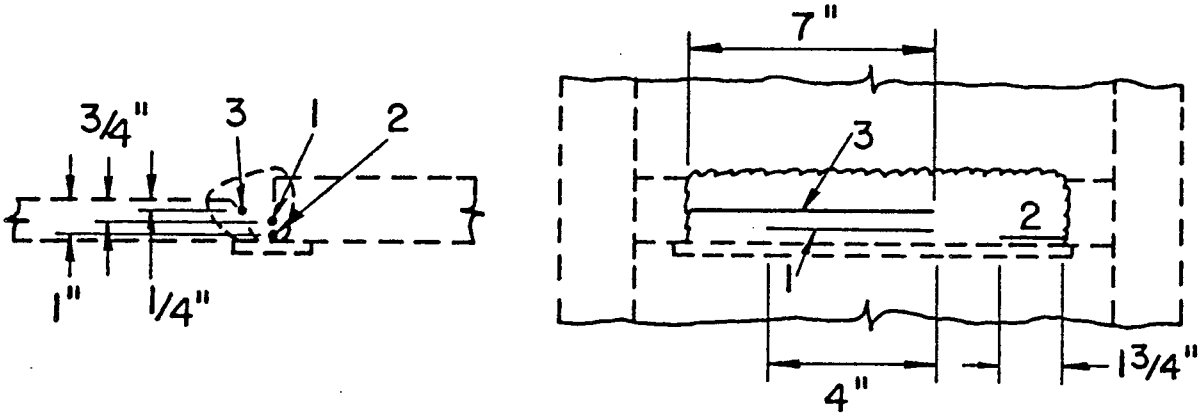

Specimen E

Figure 13: Sizes and Locations of the Groove Weld Defects in Test T6 (E)

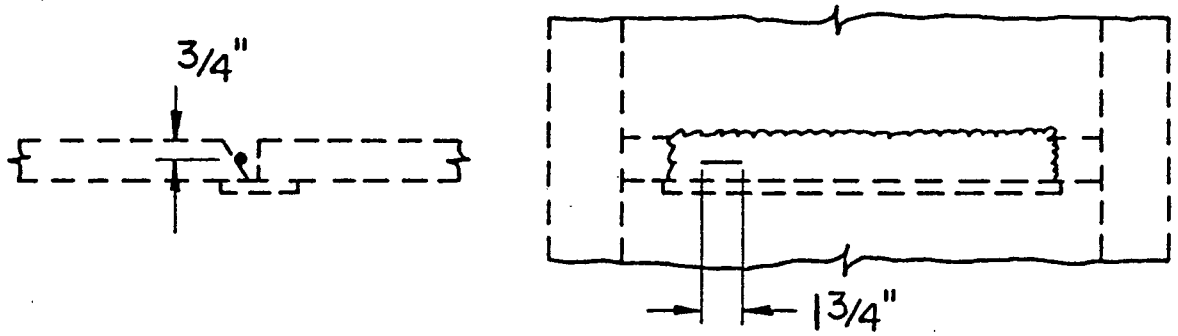

Specimen C2

Figure 14: Sizes and Locations of the Groove Weld Defects in Test T10 (C2)

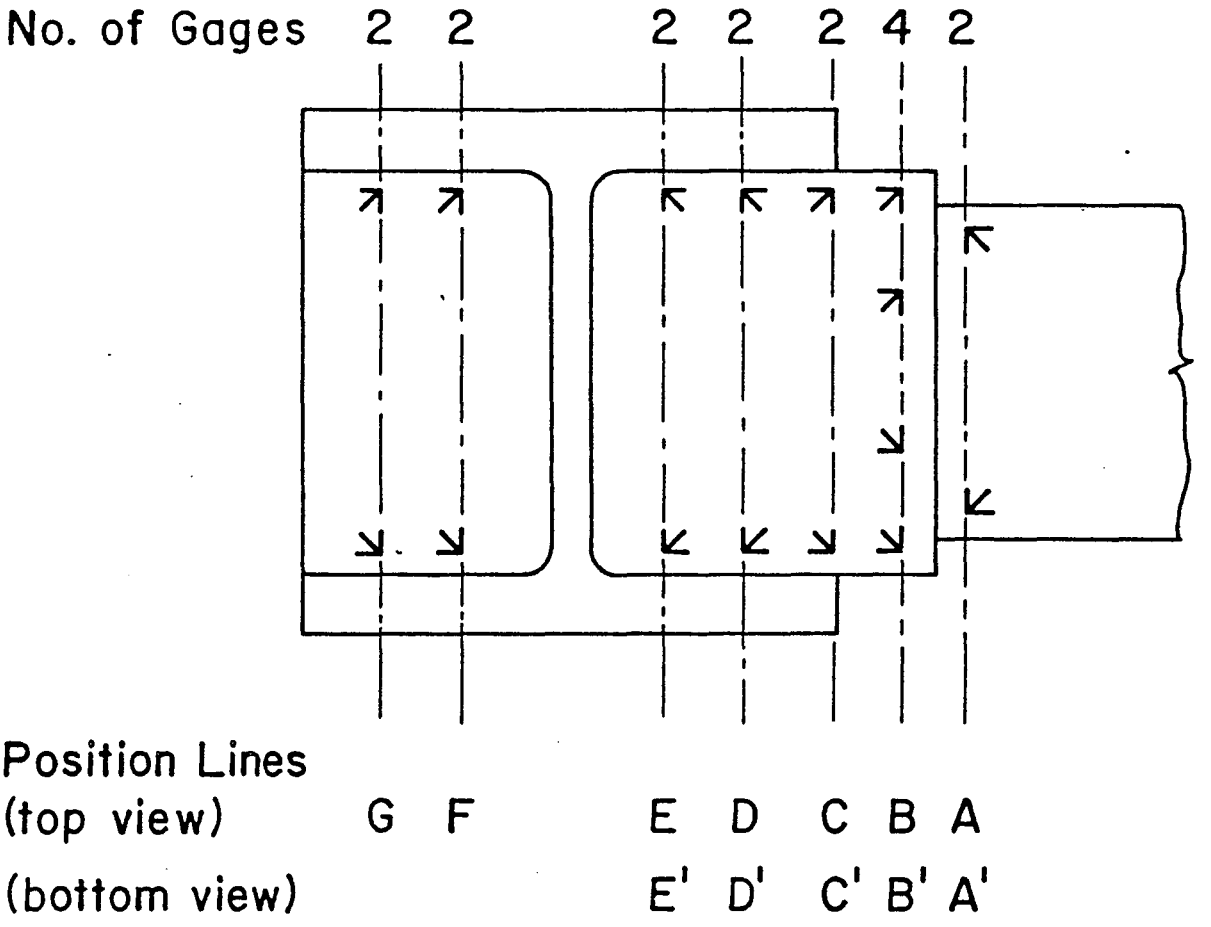

Bottom View : Refers to the side with backing bar.

Figure 15: Sketch of Rosette Layouts

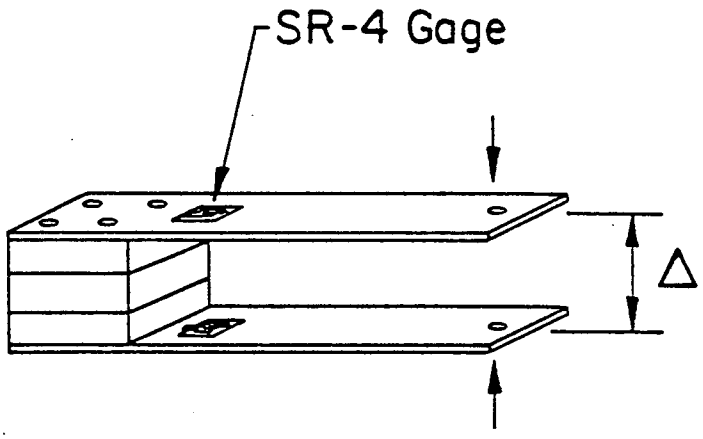

DEFLECTION GAGE
(cantilever gage)

Figure 16: An Overall View of a Cantilever Gage

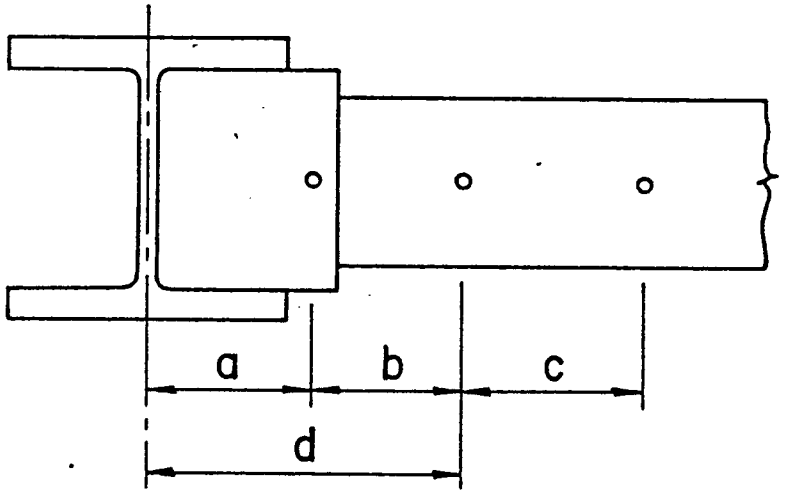

Figure 17: Locations of the Gage Lengths

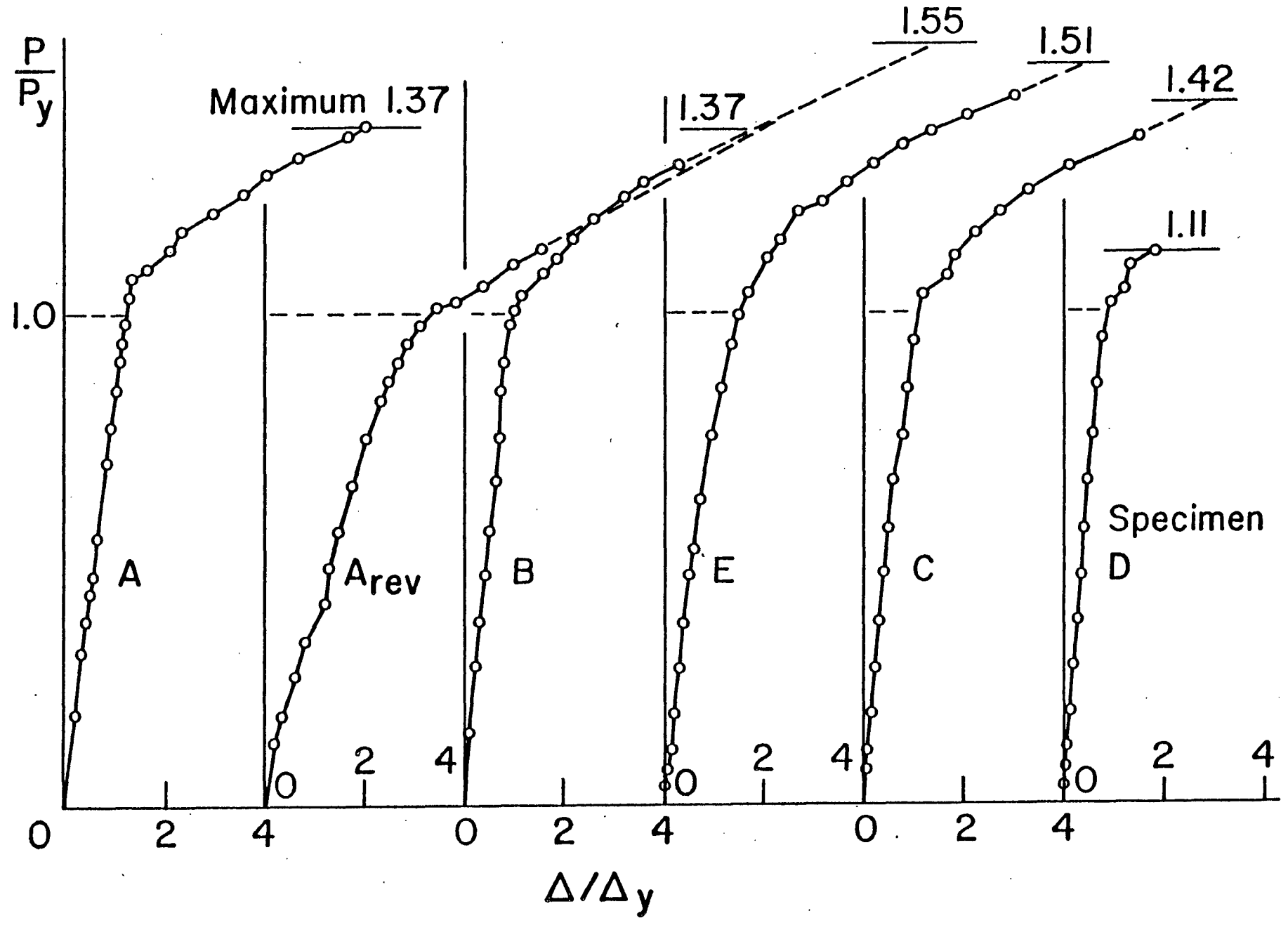

Figure 18: Load-Deflection Curve of First Six Tests

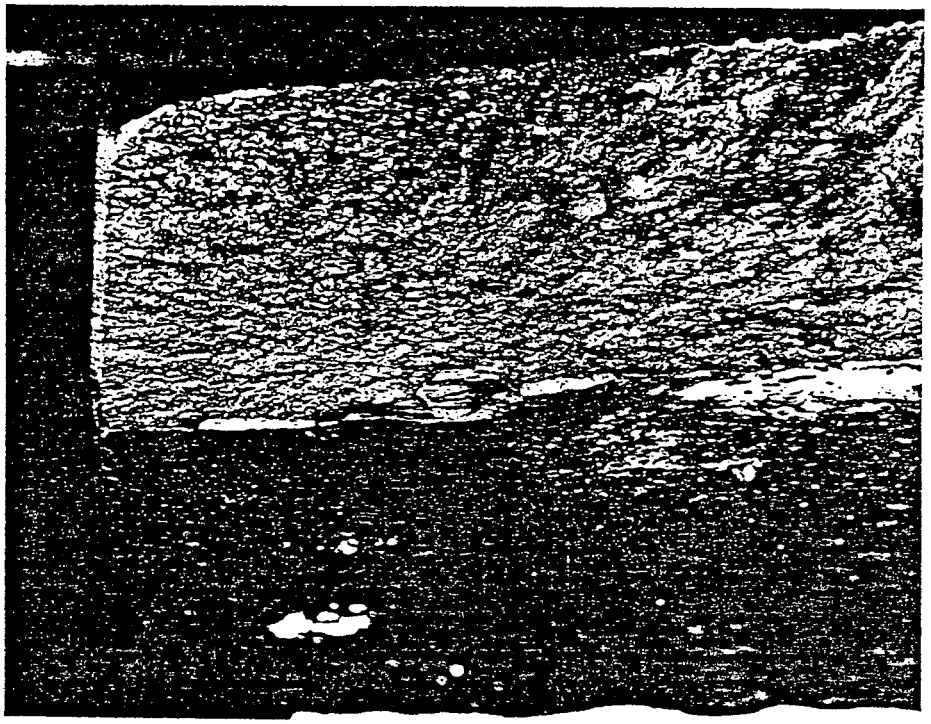

Figure 19: Fracture Surface of Test T1

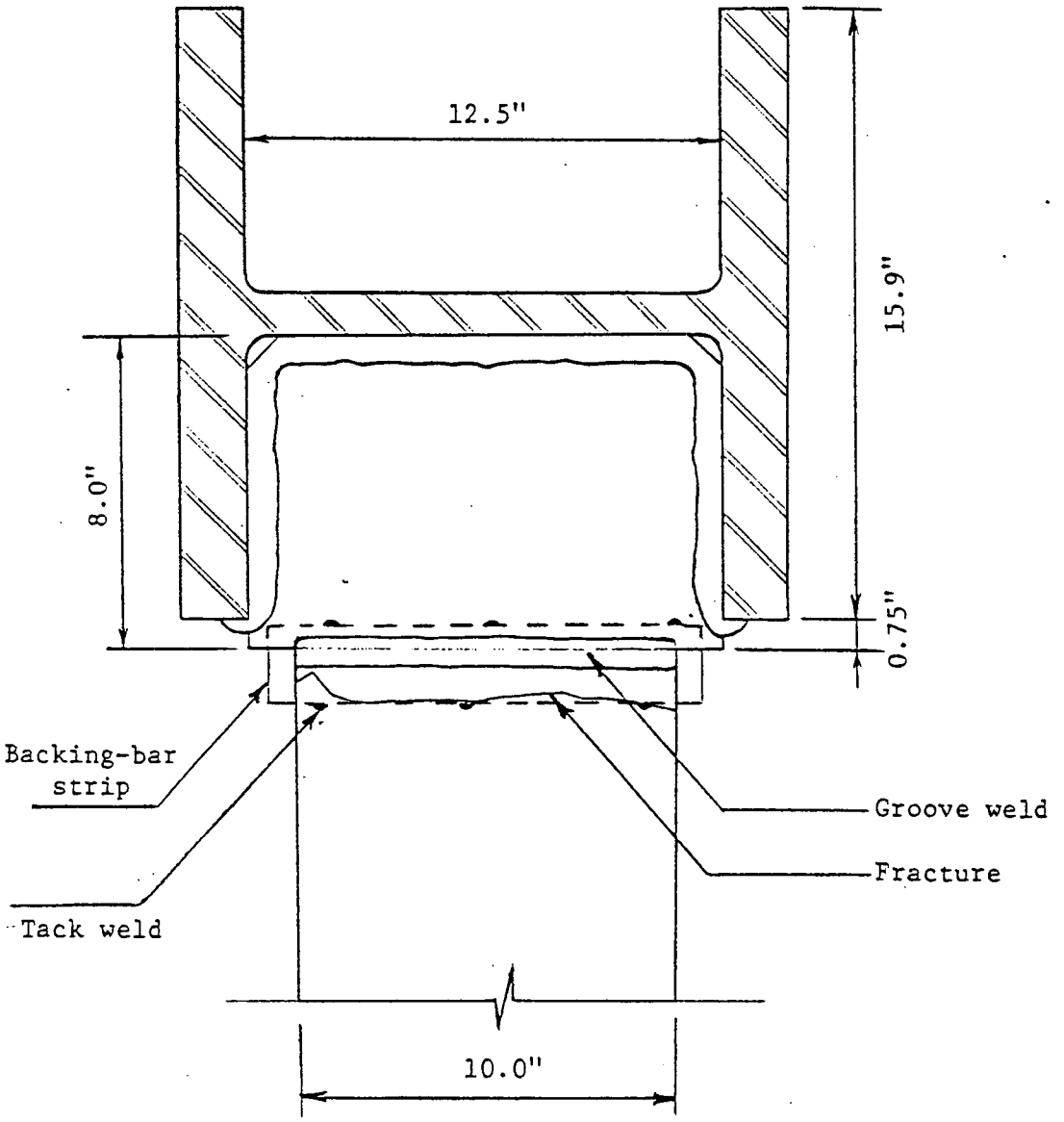

Figure 20: Fracture Trace of Test T1

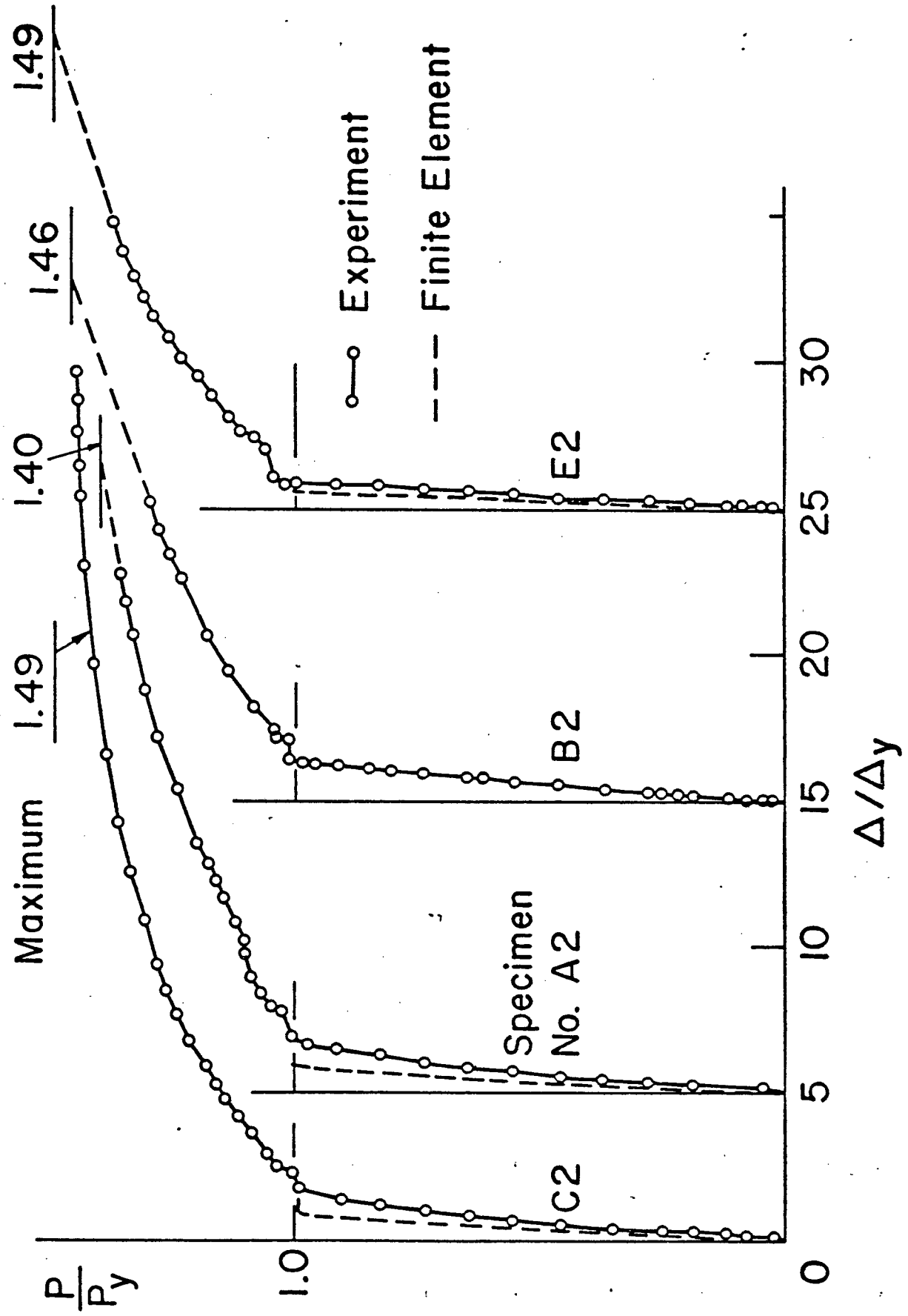

Figure 21: Load-Deflection Curve of Last Four Tests

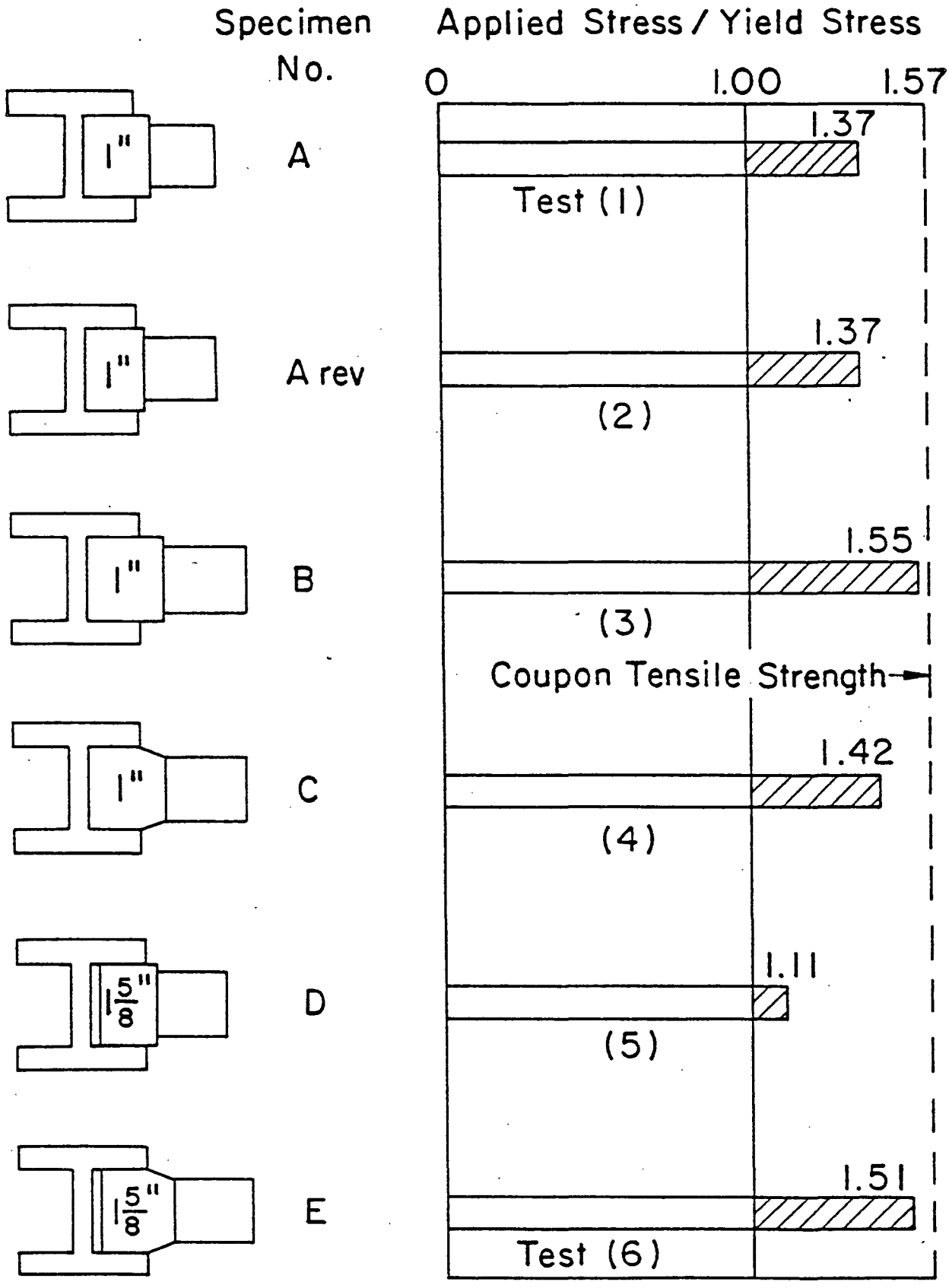

Figure 22: Details Tested in First Six Tests

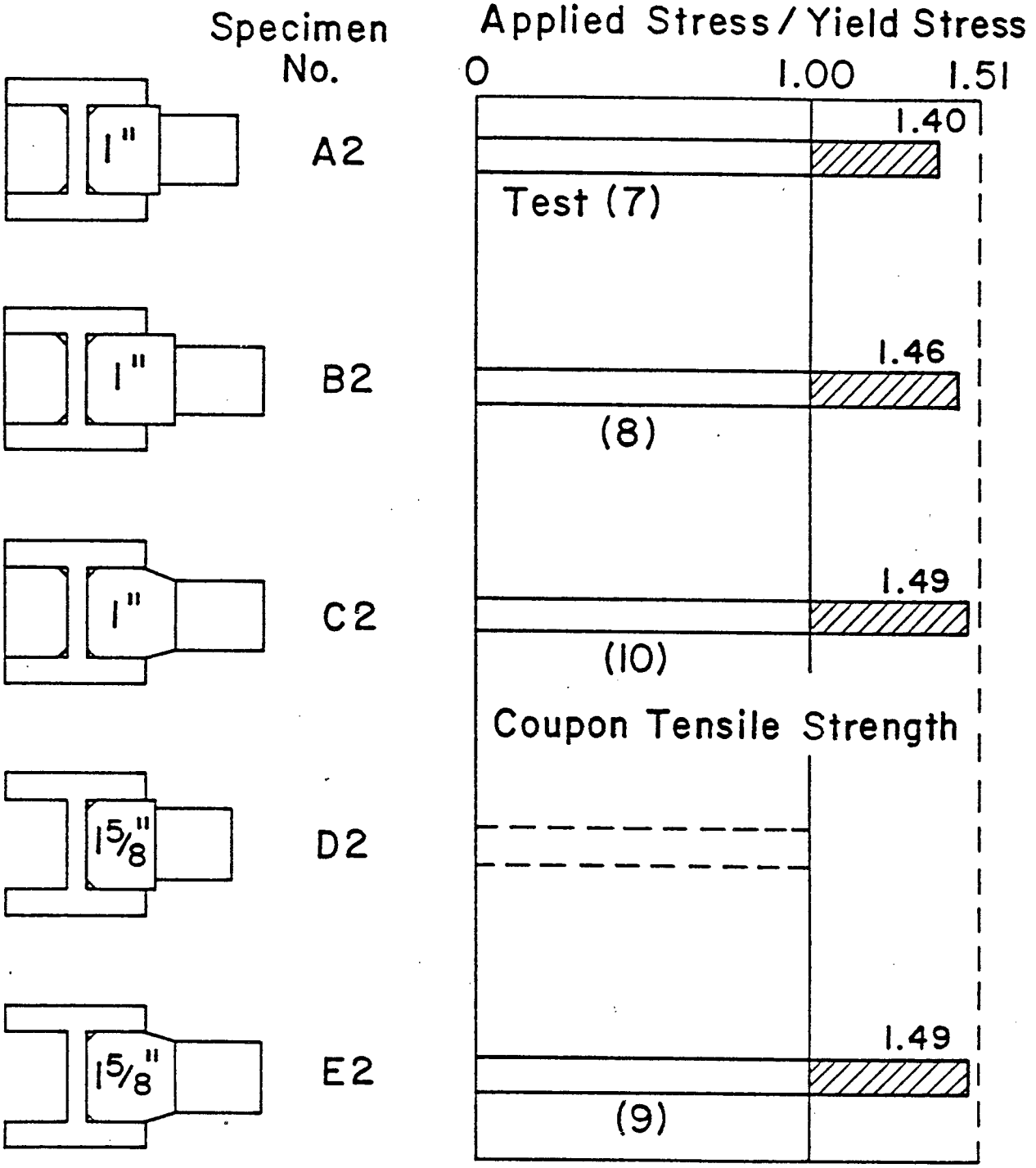

Figure 23: Details Tested in Last Four Tests

11 REFERENCES

American Welding Society 1980
STRUCTURAL WELDING CODE.American Welding Society

Bathe, K. J., Wilson, E. L., and Iding, R. H. 1974
NONSAP -- A STRUCTURAL ANALYSIS PROGRAM FOR STATIC AND DYNAMIC RESPONSE OF LINEAR SYSTEMS. SESM Report 74-3, University of California, Berkeley.

Driscoll, G.C. 1979
FRACTURES OF BEAM-TO-COLUMN WEB MOMENT CONNECTIONS. Fritz Engineering Laboratory Report 405.10, Lehigh University.

Munse, W.H., and Chesson, E. 1963
RIVETED AND BOLTED JOINTS: NET SECTION DESIGN. Journal of the Structural Division, ASCE 89(ST1).

Novak, S. R. 1974
RESISTANCE TO PLANE-STRESS FRACTURE (R-CURVE BEHAVIOR) OF A572 STRUCTURAL STEEL. Special Technical Publication STP 591, American Society for Testing Materials.

Popov, Egor P. and Pinkney, R. Bruce 1969
CYCLIC YIELD REVERSAL IN STEEL BUILDING CONNECTIONS. Journal of the Structural Division, ASCE 95(ST3):327-353.
Also printed, Engineering Journal, AISC, Vol. 8, No. 3, July 1971, pp. 66-79.

Rentschler, G.P., Chen, W.F., Driscoll, G.C. 1980
TESTS OF BEAM-TO-COLUMN WEB MOMENT CONNECTIONS. American Society of Civil Engineers Proceedings, 106(ST5):1005-1022.
Fritz Engineering Laboratory Report No. 405.7.

Shen, Shi-Zhao, and Driscoll, G. C. 1981a
PARAMETRIC ANALYSIS OF TENSION FLANGE CONNECTION DETAILS. Fritz Engineering Laboratory Report 469.3, Lehigh University.

Shen, Shi-Zhao, Pourbohloul, Abbas, Haist, Randall M., and Driscoll, George C. 1981b
ELASTIC-PLASTIC ANALYSIS OF TENSION FLANGE CONNECTION DETAILS. Fritz Engineering Laboratory Report 469.4, Lehigh University.